

Review

Conductive Molecularly Imprinted Polymers (cMIPs): Rising and Versatile Key Elements in Chemical Sensing

Adriana Feldner ^{1,2,3} , Julia Völkle ^{1,2,3}, Peter Lieberzeit ^{2,3}  and Philipp Fruhmann ^{1,*} 

¹ Centre of Electrochemical Surface Technology, Viktor-Kaplan-Straße 2, 2700 Wiener Neustadt, Austria; adriana.feldner@cest.at (A.F.); julia.voelkle@cest.at (J.V.)

² Department of Physical Chemistry, Faculty for Chemistry, University of Vienna, Währinger Straße. 42, 1090 Vienna, Austria; peter.lieberzeit@univie.ac.at

³ Vienna Doctoral School in Chemistry (DoSChem), University of Vienna, Währinger Straße. 42, 1090 Vienna, Austria

* Correspondence: philipp.fruhmann@cest.at

Abstract: Molecularly imprinted polymers (MIPs) have proven useful as receptor materials in chemical sensing and have been reported for a wide range of applications. Based on their simplicity and stability compared to other receptor types, they bear huge application potential related to ongoing digitalization. This is the case especially for conductive molecularly imprinted polymers (cMIPs), which allow easy connection to commercially available sensing platforms; thus, they do not require complex measuring setups. This review provides an overview of the different synthetic approaches toward cMIPs and the obtained limit of detections (LODs) with different transducing systems. In addition, it presents and discusses their use in different application areas to provide a detailed overview of the challenges and possibilities related to cMIP-based sensing systems.

Keywords: molecularly imprinted polymers; conductive polymers; sensors; electropolymerization; composites



Citation: Feldner, A.; Völkle, J.; Lieberzeit, P.; Fruhmann, P. Conductive Molecularly Imprinted Polymers (cMIPs): Rising and Versatile Key Elements in Chemical Sensing. *Chemosensors* **2023**, *11*, 299. <https://doi.org/10.3390/chemosensors11050299>

Academic Editors: Daniele Merli and Giancarla Alberti

Received: 31 March 2023

Revised: 12 May 2023

Accepted: 15 May 2023

Published: 18 May 2023



Copyright: © 2023 by the authors. Licensee MDPI, Basel, Switzerland. This article is an open access article distributed under the terms and conditions of the Creative Commons Attribution (CC BY) license (<https://creativecommons.org/licenses/by/4.0/>).

1. Introduction

Molecularly imprinted polymers (MIPs) are synthetic materials that mimic the selective interaction of biological receptors to their substrates and are therefore often referred to as artificial antibodies. Compared to biomolecules, MIPs have several advantages ranging from better stability in various media and larger tolerance regarding temperature and pH to improved storage and reusability. Additionally, it is cheaper to produce them; the process is scalable and can be adjusted to a wide range of applications [1–3]. Molecular imprinting results in binding sites that are complementary to the analyte in size and shape. Functional monomers are capable of interacting with the template and polymerize around it, while a cross-linker stabilizes the matrix (Figure 1).

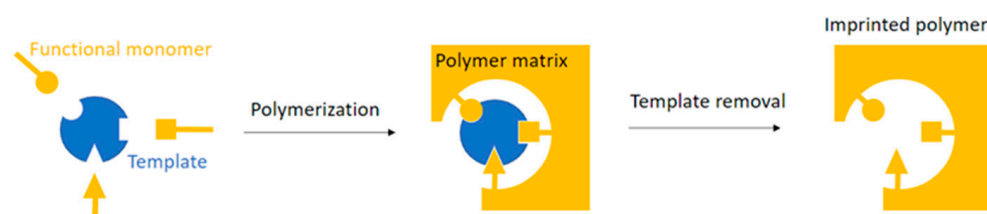


Figure 1. Molecular imprinting: First functional monomers self-assemble around the template according to their functional groups. During polymerization with a cross-linker, a stable matrix forms around the template. After template removal, the imprinted polymer remains.

After template removal, stable cavities remain in the polymer that can selectively rebind the target analyte. MIPs can be synthesized in several shapes such as thin films [4]

or particles [5]. Molecular imprinting is a highly useful technique and develops rapidly due to improved fabrication techniques such as solid phase synthesis as well as their huge application potential in sensing [6–10]. By definition, a chemical sensor is a “device that transforms chemical information ranging from the concentration of a specific sample component to total composition analysis, into an analytically useful signal. The chemical information, mentioned above, may originate from a chemical reaction of the analyte or from a physical property of the system investigated” [11].

In general, sensors are small, inexpensive, and portable devices that do not require a large laboratory. Ideally, a sensor should provide high selectivity and sensitivity as well as stability and reproducibility. Every sensor consists of two main parts: receptor and transducer. The receptor selectively recognizes and binds the analyte, whereas the transducer transforms the information from the binding event into a measurable signal [11]. Figure 2 shows a typical chemical sensor. In general, sensors can be classified according to their transducers, which typically are optical, electrochemical, or mass-sensitive devices [12].

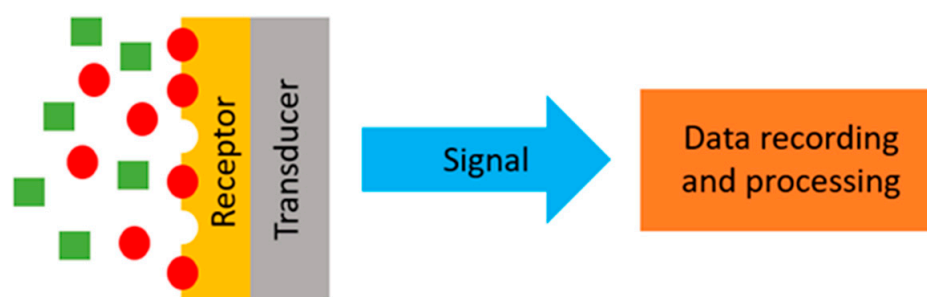


Figure 2. A chemical sensor consisting of a receptor layer and a transducer. The receptor only binds the analyte (red spheres). The interfering substance (green rectangles) do not fit into the cavities. The signal is forwarded to a data processing unit.

From a historic perspective, MIP synthesis originally focused on electrically insulating materials. Early research on imprinted silica gel [13,14] was followed by extensive investigations on a wide range of organic polymers in the 1970s [1]. To date, vinyl, acrylate, and silane-based polymers are among the most commonly used for MIP synthesis [15]. With the emergence of electrically conducting polymers in the second half of the 20th century [16–18] and rapid progress in the field of conductive, high-performance polymer nanocomposites [19,20], increasing research efforts have focused on the integration of such materials into the imprinting process, yielding electrically conducting MIP-sensing layers. Although different reviews for specific applications, or sensing itself, are available, they usually do not differentiate between conductive and non-conductive MIPs [21–25]. In general, the possibility to interact with an analyte is basically the same, but the use of conductive MIPs (cMIPs) as receptors comes with the advantage of a direct electrical response upon a binding event.

Conductive polymers are a subclass of organic polymers and possess certain electrical and optical properties similar to semiconductors or metals. Usually, one can synthesize them in a simple and cost-effective way [26]. Combining conductive polymers (or their abilities) with the selective recognition of MIPs merges the advantages of two well-established techniques. This makes it possible to fabricate sensing devices, which are not available with non-conducting MIPs [27]. The cMIPs directly change their electrical properties on the binding sites upon analyte interaction and allow for direct detection of this event due to the intrinsically present conductivity. The specific binding sites of the cMIPs increase the affinity of the electrochemical sensor toward the desired analyte. The combination of cMIPs as both a receptor and an electrochemical transducer can, for example, reduce interference of structurally similar compounds, since they would not only differ in their interaction with the binding sites of the MIP but also in their electrochemical signal [28]. cMIPs present the same advantages as non-conductive MIPs compared to conventional receptors

of electrochemical sensors. They are more stable in different media and temperatures than biomolecules such as antibodies. Furthermore, their preparation is faster and cheaper than antibody culturing. Additionally, cost- and time-expensive cell and animal culturing is not necessary for cMIP synthesis [29]. cMIP sensors can be prepared for analytes in liquid as well as in gas phase. For gaseous analytes, resistive devices are often used. They have the advantage that they do not need to be heated to high temperatures as is the case for semiconductor metal oxide sensors [30]. In spite of all their beneficial properties and remarkable achievements in the last years, imprinted polymer-based systems are usually still not as common and sensitive as chromatographic methods. Although this is a crucial issue in trace analysis, the simplicity, cost efficiency, and versatile application potential of molecularly imprinted polymers are outstanding and will promote their implementation in analytical devices in the future.

For this reason, this review aims to provide an overview of the use of cMIPs as receptor materials and their application possibilities in chemical sensing over the last 20 years. The main part of this review focuses on the different monomers and systems to obtain cMIPs and provides an overview of analytes and LODs. Later, it discusses how to couple them to different transducer types and briefly discusses application areas to summarize the usability and potential of cMIPs in chemical sensing.

2. Conductive MIPs

This section is divided into five subsections based on the respective monomers to obtain the corresponding conductive MIPs (Figure 3).

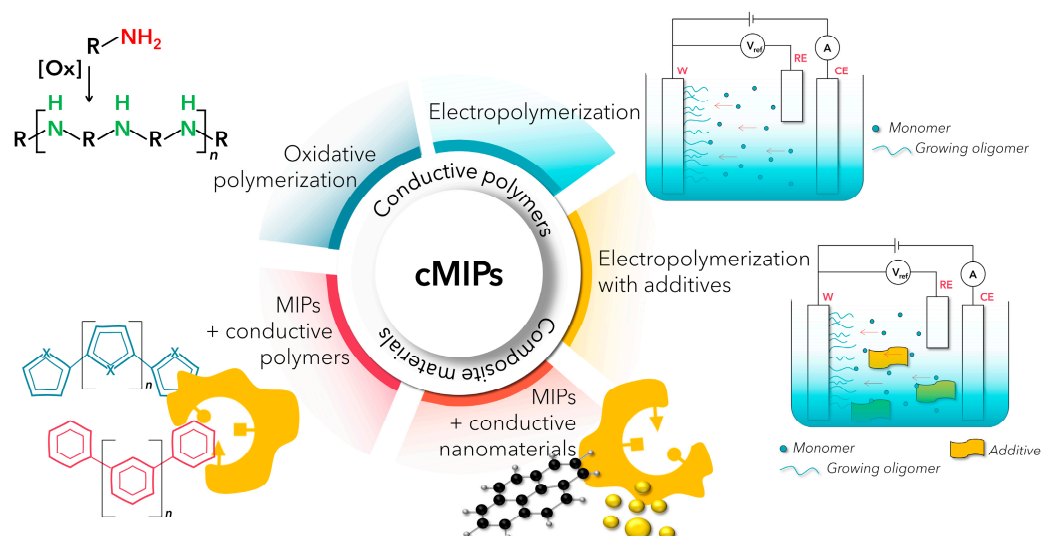


Figure 3. Conductive molecularly imprinted polymers (cMIPs) can be divided into different subcategories based on their fabrication process.

2.1. Electropolymerization

Electropolymerization is the classical and most straightforward way to obtain cMIPs. This technique leads to a thin polymer film directly on the electrode. The template is usually added to the monomer solution and is incorporated by the polymer matrix. Polymerization proceeds by applying electrochemical methods, such as cyclic voltammetry (CV) or chronoamperometry. The amount of charge transferred during synthesis controls the film thickness. However, electropolymerization requires the presence of electroactive moieties in the monomers. Hence, pyrrole, aniline, and 3-aminophenylboronic acid are among the most frequently used monomers for that purpose [31].

2.1.1. Pyrrole

Polypyrrole (PPy) does not require any additives to introduce conductivity, since it is intrinsically a conductive polymer. Based on this, pyrrole has been widely used to prepare cMIPs targeting small molecules up to large biomolecules and microorganisms. Successful imprinting of the first class, among others, include small bioactive molecules, such as the antibiotic doxycycline and the antimicrobial drug sulfadimethoxine [32]. Two different approaches are described for sulfadimethoxine, where the earlier report focuses on preparing microstructured PPy cMIPs on micromachined silicon using light-activated electropolymerization. The approach results in an LOD of around 1 mmol/L [33]. By focusing on the different imprinting parameters, Turco et al. successfully improved the LOD with a similar system to 70 $\mu\text{mol/L}$. In addition, they demonstrated that the cationic electrolyte has a significant influence on MIP morphology [34]. Other examples of small-molecule cMIP are the successful imprinting of L-tryptophan [35] and caffeine [36]. It was demonstrated that pyrrole is the better suited monomer compared to aniline, since it is more affine to L-tryptophan [35]. Interestingly, Choong et al. were able to demonstrate a novel application of cMIP-based caffeine sensors, in which the detection window is reversibly modulated using electrical stimuli [36]. The degree of swelling of the polymer is associated with ion transport in and out of the polymer and can be controlled electrochemically [36].

Larger biomolecules were also successfully imprinted using electropolymerization of pyrrole (Figure 4). Examples include human serum albumin (HSA) [37], bovine leukemia virus glycoprotein gp51 [38], SARS-CoV-2 spike glycoprotein [39], and hazelnut Cor a 14-allergen [40], which resulted in developing corresponding sensors. The best LODs were in the fM range for the Cor a 14 allergen using square wave voltammetry and SPR [40]. In terms of whole biological systems, Tokonami et al. used PPy to imprint different gram-positive (*Bacillus subtilis*, *Staphylococcus aureus*) and gram-negative (*Escherichia coli*, *Pseudomonas aeruginosa*) bacteria on thin films [41]. Jamieson et al. presented a different approach using the heat-transfer method, which monitors changes in thermal resistance to detect microorganisms; this was successfully achieved for yeast [42].

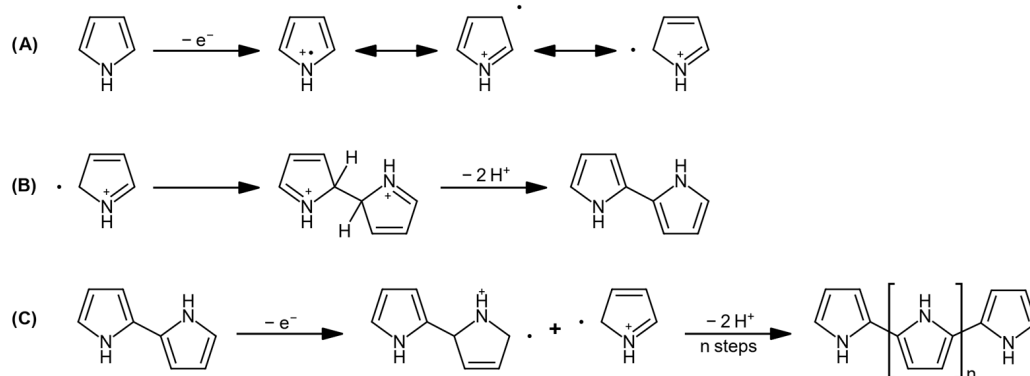


Figure 4. Synthesis of PPy as general example for an electropolymerization process. Key steps are (A) pyrrole oxidation, (B) dimer formation, and (C) coupling and final rearomatization. The depicted mechanism is very similar for thiophene and aniline.

Although electropolymerization of pure pyrrole often leads to satisfying results, one can add carboxylated pyrrole monomers to increase functionality of the polymer. For example, it was demonstrated that 15 wt% pyrrole-3-carboxylic acid in a formaldehyde-imprinted PPy is beneficial for the system, since the acid group can better interact with the template through hydrogen bonds [43]. This cMIP was successfully applied to chemiresistors [44] and optical fibers [43,44]. Silva et al. developed a sensor for cardiac troponin T by focusing on various ratios and combinations of the monomers pyrrole, pyrrole-2-carboxylic acid, and pyrrole-3-carboxylic acid. They obtained the best rebinding results using a ratio of 1:5 of pyrrole and pyrrole-3-carboxylic acid, respectively [45]. Kim et al. prepared porous poly(py-co-py-3-carbox) films on colloidal lithography gold pore arrays to detect

theophylline, demonstrating that structured cMIPs result in higher sensitivity than do planar films of the same imprinted polymer [46].

Pyrrole can also be co-polymerized with other monomers to obtain specific systems. A biochemical sensor with a new conductive ferrocenyl chalcone derivative was developed by Chen. First, they synthesized [1-oxo-3-(3-thienyl)-2-propen-1-yl] ferrocene (OTPyFc) via aldol reaction and then electropolymerized it with pyrrole to obtain a dopamine-imprinted co-polymer [47]. In addition, there is also the possibility of using PPy as a support with a different imprinted polymer on top. Rick et al. demonstrated a combination of polyaminophenylboronic acid MIP on a PPy supporting layer. p-APBA reversibly mediates recognition of various bio-macromolecules and forms a self-doped polymer layer. The PPy interlayer improves response and sensitivity [48].

2.1.2. Aniline

Although PPy is the most used conductive polymer, polyaniline (PANI) is nearly as popular and is widely applied in electrochemistry. It has some outstanding properties such as reversible doping, good pH and environmental stability, and superior electrical conductivity [49]. PANI often forms nanofibers, which are beneficial in a variety of applications due to tunable properties and the fact that they usually have a high surface-to-volume ratio [50]. Nevertheless, aniline should be used with caution since it is a toxic compound that causes methemoglobinemia [51] and splenic toxicity [52]. Electropolymerization of aniline in the presence of bovine serum albumin (BSA) (template and analyte) led to PANI cMIP on ITO substrates [53]. Lee et al. developed a multichannel system based on PANI-co-metanilic acid for the detection of several hormones (17 β Estradiol, Cortisol, progesterone, and testosterone). PANI synthesis usually requires an acidic environment. Co-polymerizing aniline with metanilic acid forms self-doped PANI without the need to add additional acid [54]. Roy et al. presented a similar approach: polyvinylsulphonic-acid-doped PANI is imprinted with para-nitrophenol [55]. Regasa et al. combined the monomers aniline and acrylic acid to obtain an electrochemical sensor for melamine detection. The sensing material was prepared using in situ co-electropolymerization of the two monomers in the presence of melamine as the template. They attributed the sensitivity of their sensor to the ability of the polymer to form multiple non-covalent interactions with the template via the amine functionality of aniline and the carboxylic group of acrylic acid, respectively [56].

2.1.3. Thiophene Derivatives

Thiophene derivatives are the third type of commonly used monomers for cMIPs [27]. Although they belong to the same chemical family, nearly every described sensing application uses a different monomer. Lattach et al. used 3,4-ethylenedioxythiophene (EDOT) and 3-acetic acid thiophene as functional monomer for atrazine-imprinted polymers [57]. Lee et al. polymerized EDOT and hydroxymethyl EDOT (EDOT-OH) in varying combinations. In the presence of the template α -synuclein peptide (Parkinson's disease marker), the polymer formed tubular nanostructures. The results were in good agreement with those obtained using enzyme-linked immunosorbent assay (ELISA) [58]. Lach et al. electropolymerized 2,2'-bithiophene-5-carboxylic acid for electrochemical detection of p-synephrine, a dietary supplement for weight loss [59]. Ayerdurai et al. developed a sensor for tyramine by electropolymerizing the functional monomers 2,20-bithiophene-5-carboxylic acid and p-bis(2,20-bithien-5-yl)-methylbenzo-18-crown-6. Introducing a functional monomer containing a crown ether moiety significantly increased selectivity of the sensor compared to sensors coated with the polymer without crown ether. The latter also reacted to interfering substances, such as glucose, urea, and creatinine [60]. Yang et al. used a very different approach: they first synthesized poly(γ -glutamic acid) modified with 3-aminothiophene co-polymer (ATh- γ -PGA). Then they prepared lysozyme-imprinted ATh- γ -PGA NPs using self-assembly and immobilized it on the electrode by electropolymerizing the thiophene groups [61]. Sharma et al. synthesized the functional monomer 4-bis(2,2'-bithien-5-yl)methylbenzoic acid glycol ester and successfully prepared an im-

printed polymer via electropolymerization in the presence of oxytocin nonapeptide, an autism biomarker [62].

2.1.4. Alternative Monomers

Phenylene diamine is a less frequent monomer. Soysal demonstrated an electrochemical sensor based on electropolymerized p-phenylenediamine MIP to detect methyl paraben [63]. Ayankojo et al. electropolymerized erythromycin-imprinted poly-phenylenediamine onto screen-printed electrodes. The functional monomer was chosen based on calculating binding energies toward the template and stability of the resulting polymer film [64]. The same group developed a similar sensor for sulfamethizole. They first optimized the MIP on surface acoustic wave (SAW) sensors and successfully transferred it to screen-printed electrodes for electrochemical measurements [65]. In addition to the monomer classes introduced thus far, there are a few examples of alternative monomers (Table 1).

Table 1. Overview: cMIP sensors prepared using electropolymerization. All LOD values were converted into mol/L (if possible) to allow for better comparison. DPV = differential pulse voltammetry, EIS = electrochemical impedance spectroscopy, CFU = colony forming unit, QCM = quartz crystal microbalance, SWV = square wave voltammetry, SPR = surface plasmon resonance, CV = cyclic voltammetry, SAW = surface acoustic wave, EG-FET = extended-gate field-effect transistor, ECS = electrochemical capacitance spectroscopy.

Monomer	Analyte	Transducer	LOD [mol/L]	Ref.
Pyrrole	Doxycycline	DPV	44×10^{-6}	[32]
Pyrrole	Sulfadimethoxine	Amperometric	0.5×10^{-3}	[33]
Pyrrole	Sulfadimethoxine	Amperometric	70×10^{-6}	[34]
Pyrrole	L-tryptophan	DPV	17×10^{-6}	[35]
Pyrrole	Caffeine	Pulsed potential	10×10^{-6}	[36]
Pyrrole	HSA	DPV	0.25×10^{-9}	[37]
		EIS	12.1×10^{-6}	
Pyrrole	Glycoprotein (<i>gp51</i>) (bovine leukemia virus)	Pulsed amperometry	$\sim 20 \times 10^{-6}$ B	[38]
Pyrrole	SARS-CoV-2 spike glycoprotein	Pulsed amperometry	12×10^{-9} B	[39]
Pyrrole	Hazel nut Cor a 14-allergen	SWV	$\sim 1.6 \times 10^{-15}$	[40]
		SPR	$\sim 1.2 \times 10^{-15}$	
Pyrrole	Bacteria	QCM	1×10^9 CFU/mL ^A	[41]
Pyrrole	Yeast	Thermal resistance	$10^{1.25} \pm 0.09$ CFU/mL	[42]
Pyrrole, pyrrole-3-carboxylic acid	Formaldehyde	Resistive and optical fiber	~ 7 ppm (res.)	[43,44]
			4.25 ppm (opt.) ^B	
Pyrrole, pyrrole-3-carboxylic acid	Cardiac troponin T	DPV	0.25×10^{-12}	[45]
Pyrrole, pyrrole-3-carboxylic acid	Theophylline	QCM	–	[46]
OTPyFc, pyrrole	Dopamine	DPV	1.7×10^{-6} D	[47]
Aminophenylboronic acid	Lysozyme/cytochrome c	CV	7×10^{-9} (lys.) ^B	[48]
Aniline	BSA Cortisol, progesterone, testosterone, 17 β -estradiol	DPV	0.59×10^{-6}	[53]
			C: 5.52×10^{-18}	
			T: 34.67×10^{-18}	
			P: 7.95×10^{-18}	
Aniline, metanilic acid	17 β -estradiol	CV	E: 33.03×10^{-18}	[54]
Aniline, polyvinylsulphonic acid	p-nitrophenol	DPV	1×10^{-6}	[55]
Aniline, acrylic acid	Melamine	DPV	17.2×10^{-3}	[56]
3-acetic acid thiophene, EDOT	Atrazine	CV	1.0×10^{-9}	[57]
Poly(hydroxymethyl 3,4-ethylenedioxythiophene)	α -synuclein	CV	6.5×10^{-15}	[58]
2,2'-bithiophene-5-carboxylic acid	p-syneprine	DPV	12.2×10^{-9}	[59]
		EIS	5.7×10^{-9}	
2,20-bithiophene-5-carboxylic acid and p-bis(2,20-bithien-5-yl)- methylbenzo-18-crown-6	Tyramine	DPV	159×10^{-6}	[60]

Table 1. Cont.

Monomer	Analyte	Transducer	LOD [mol/L]	Ref.
3-aminothiophene, ATh- γ -PGA	Lysozyme	DPV	0.1×10^{-9} ^B	[61]
4-bis(2,2'-bithien-5-yl)methyl- benzoic acid glycol ester	Oxytocin nonapeptide	EIS	60×10^{-6}	[62]
p-phenylenediamine	Methyl paraben	DPV	10×10^{-6}	[63]
m-phenylenediamine	Erythromycin	DPV	0.1×10^{-9}	[64]
m-phenylenediamine	Sulfamethizole	SAW/DPV	0.9×10^{-9} (DPV)	[65]
Triphenylamine rhodanine- 3-acetic acid	Metalloproteinase-1 (MMP-1)	EG-FET	20×10^{-9} (epitope 1) 60×10^{-9} (epitope 2)	[66]
Toluidine blue	Prostate specific antigen (PSA)	DPV	29.4×10^{-15} ^C	[67]
Bismarck Brown Y	Uric acid	EIS/ECS	0.160×10^{-6}	[68]

^A No LOD given. Only one concentration measured. ^B No LOD given. Lowest concentration of calibration curve. ^C No LOD given. Lower limit of quantification. ^D No LOD given. Lowest concentration of linear range.

These reports include the use of triphenylamine rhodanine-3-acetic acid to imprint two epitopes of matrix metalloproteinase-1, which is a biomarker for idiopathic pulmonary fibrosis (IPF). Imprinting and sensor fabrication took place using electropolymerization on an EG-FET [66]. In addition, a few papers report using dyes for preparing cMIP. To obtain a PSA sensor, Abbasy et al. electropolymerized Toluidine Blue in a pre-formed glutaraldehyde–cysteamine matrix on a gold electrode. This increased the stability of the MIP against degradation [67]. Trevizan et al. report an electrochemical sensor for uric acid prepared using electropolymerization. The monomer in this case is the diazo dye Bismarck Brown Y. The azo group of the resulting polymer contributes to the redox capacitance of the electrode. Thus, the sensor is able to perform electrochemical measurements without the need for adding a soluble redox probe [68].

While electropolymerization of intrinsically conducting MIPs represents a straightforward method for depositing sensing layers of well-defined thickness, viscoelastic properties, and porosity directly onto the transducer substrate [31], there are several caveats to be considered. For one, the pH during electropolymerization strongly influences the final polymer product. Pyrrole polymerization for instance is severely inhibited at elevated pH [69,70], and PANI films polymerized in a basic environment display only very low conductivity [71]. This limits the pH range at which cMIP synthesis can take place and can result in reduced selectivity, as the net charge of the template also changes with pH. Most amino acids, for instance, are uncharged during PPy electropolymerization, resulting in low imprinting effects [31,72]. Moreover, imprinting of redox-active templates can be very challenging: electrode reactions during polymerization might result in electrode fouling and cMIP films that bind to the products of such reactions, rather than to the template itself [31]. Similar issues must be considered when synthesizing cMIPs that display electrocatalytic behavior, most prominently poly-(3,4-ethylenedioxythiophene) (PEDOT), especially when imprinting easily oxidizable molecules such as dopamine, uric acid, and ascorbic acid [73]. An approach to address these issues is the use of structural analogue templates that carry the desired charge during polymerization and are redox inactive [31,74]. Another challenge faced by PEDOT-based sensing layers in particular is the polymers' high hygroscopicity. Swelling and collapsing upon fluctuations in ambient humidity result in significant alterations of the polymers' electric conductivity unrelated to specific analyte interactions [75]. In order to reduce such humidity-induced changes, hydrophobic additives can be included in the imprinting protocol [76]. Further possible benefits of incorporating additives during MIP electrodeposition are discussed in the following section. Table 1 provides a detailed overview of the cMIP sensors prepared by electropolymerization of the different monomers.

2.2. Electropolymerization + Additives

To enhance certain properties, electropolymerized MIPs can be combined with a wide range of additives. For example, the electrical response can be further increased by introducing 2D materials such as graphene [77,78], carbon nanotubes (CNTs) [79,80], or MXenes [81]. Additives such as nanoparticles [82–84] can also increase affinity toward the analyte and enhance sensitivity by increasing the active surface area.

2.2.1. Systems Based on Polypyrrole

Even though PPy is a conductive polymer, it is often combined with additives to adjust the properties of the system. Ma et al. prepared a porous MXene/NH₂-CNTs composite combined with PPy MIP to detect fisetin. The NH₂-CNTs served as an interlayer spacer; they formed a porous structure and enhanced both surface area and electrical conductivity. Fisetin is a flavonoid and a strong antioxidant. In this study, the researchers optimized several parameters, including film thickness, monomer-to-template ratio, and extraction time, to obtain maximum sensitivity. The results were in good agreement with HPLC [81]. Duan et al. electropolymerized cysteine-imprinted PPy on glassy carbon (GC) electrodes modified with Prussian-Blue-porous carbon-CNT hybrids to enhance the surface area. Prussian Blue acts as the electric mediator. This resulted in a 3D-porous sensor that can enantioselectively recognize L- and D-cysteine and reaches better LOD values than previously reported methods of cysteine sensing [85]. In a similar approach, Rezaei et al. prepared a caffeine-imprinted nanocomposite based on PPy, sol-gel matrix, and gold nanoparticles (AuNPs). The AuNPs serve for amplifying the electrical response of the sensor [86]. To fabricate a ricin toxin chain A sensor, Komarova et al. used pyrrole and macromolecular dopants with strong protein affinity (Ponceau S, Coomassie BB R250 and ι -Carrageenan). Their approach relies on the concept of substrate-guided dopant immobilization with subsequent formation of the polymer film. In this proof-of-concept work, they obtained the best results with Coomassie BB with LOD values comparable to those of ELISA [87]. For detecting tyrosine, Saumya et al. developed a voltammetric sensor based on in situ copper-oxide-modified PPy MIP. They deposited copper on the MIP from CuCl₂ solutions and then scanned anodically in NaOH medium. The resulting sensor exhibits higher sensitivity than the corresponding version comprising other metal oxides [88]. Yin et al. demonstrated an electrochemical cadmium sensor by electropolymerizing pyrrole on carbon-disulfide-functionalized graphene oxide (GOCS) composite. The resulting sensor exhibits large specific surface area and high conductivity of the GOCS composite. The sensor is capable of detecting trace cadmium ions in fruit and vegetable samples [77]. A different type of heavy metal sensor was demonstrated by Mao et al. who used nanobiochar as the conductive material and electropolymerized L-cysteine as the selective recognition element for Pb²⁺ and Cd²⁺ [89]. Ma et al. presented a sensing platform for dopamine detection. They used multi-walled carbon nanotube (MWCNT)-spaced graphene aerogels and imprinted PPy. The CNTs enhanced the conductivity and electrochemical performance of the sensor, while the loose aerogel structure increased the effective surface area [79]. Bai et al. demonstrated an electrochemical MIP sensor for olaquinox detection. They electropolymerized pyrrole on dopamine-functionalized graphene, which improves the conductivity of the system. Dopamine was added to enhance both dispersion and adhesion of graphene. The results obtained with this sensor are in good agreement with results from high performance liquid chromatography (HPLC) [78].

2.2.2. Aniline-Based Systems

Lee et al. prepared PANI-co-metaniolic acid doped with tungsten disulfide (WS₂) imprinted with 17 β Estradiol. Adding WS₂ led to higher electrochemical responses compared to pure MIP sensors. Transition metal dichalcogenides have direct band gaps and enhance the electrochemical signal of the sensor [90]. Essoussi et al. electropolymerized nitrate-imprinted PANI on copper nanoparticles to modify GC electrodes. The nanoparticles improve sensitivity and selectivity [83]. Pandey et al. prepared a chiral selective conductive

polymer nanocomposite. For sensing D- and L-ascorbic acid, they synthesized imprinted PANI–ferrocene–sulfonic acid films on the surfaces of c-dot-modified electrodes. The sensor can discriminate and detect the chiral analytes [91]. Lee et al. synthesized three novel peptides and used them as templates for epitope imprinting. The target analyte was C-reactive protein, which is related to cardiovascular disease, fibrosis, cancer, and viral infections. They electropolymerized various ratios of aniline and m-aminobenzenesulfonic acid to obtain maximum electrochemical response. Additionally, they doped the MIPs with MXenes (Ti_2C). This increased the sensing range from 0.1 to 100 fg/mL up to 10,000 fg/mL. The sensor responses were amplified by a factor of 1.3 within the sensing range [92]. Phonklam et al. demonstrated a sensor for cardiac troponin. For that, they electropolymerized aniline on MWCNTs functionalized with a polymethylene blue redox probe [93]. Yarkaeva et al. developed an amoxicillin sensor based on two different imprinted polymers: they electropolymerized aniline and 2-methoxyaniline, respectively. The latter sensor showed higher selectivity toward the desired analyte compared to similar antibiotics [94].

Truta et al. prepared antigen-imprinted aminophenol sensors using the advantages of low cost and rapid manufacturing among others. According to the researchers, these sensors may be an alternative to immunoassays based on antibodies. In addition, they claim that the system is potentially useful for any other target [95]. Zhang et al. developed an electrochemiluminescence sensor to detect prometryn. First, they deposited perovskite quantum dots on the electrode and then coated them with electropolymerized imprinted poly-aminophenol [96]. Teng et al. synthesized imprinted o-phenylenediamine on a layer of conductive poly(p-aminobenzene sulfonic acid) for paracetamol detection [97]. A sensor for detecting tetracycline residues in food samples was presented by Abera et al. The researchers modified a CO_2 -laser-induced graphene electrode with AuNPs and an MIP based on electropolymerized o-phenylenediamine. They tested the sensor in milk and meat samples. The researchers claim that their system presents an improvement to state-of-the-art sensors for this compound in terms of sensitivity [98]. Tang et al. prepared nanocomposites based on upconverting a nanoparticle functional zeolite imidazolate framework (UCNPs@ZIF-8) and o-phenylenediamine MIP for imidacloprid [99]. Wang et al. developed a sensor for enrofloxacin detection based on o-phenylenediamine MIP together with mercaptopropionic-acid-functionalized copper nanoclusters (MPA-Cu NCs) [100]. Mahmoud et al. polymerized polyaminothiophenol (p-ATP) on N,S co-doped graphene quantum dots (GQD) in the presence of AuNPs. This led to the formation of an Au-S-covalent network. The quantum dots improve the electron transfer rate, enhance surface activity, and amplify the signal. The presence of hydrophobic and hydrophilic planes in GQDs enhances analyte adsorption and provides charge transport pathways to the electrode. Additionally, they interact with p-ATP by π - π stacking. Doping with N and S enhances conductivity. AuNPs amplify the signal [84]. Xie et al. prepared a AuNP-GC electrode modified with p-ATP. They synthesized the polymer, which they imprinted with chlorpyrifos directly on the electrode via CV. The response of the imprinted p-ATP-AuNP-GC sensor to the analyte is 3.2-fold compared to the p-ATP-Au sensor [101]. Wang et al. used self-assembly of p-ATP on a gold electrode. The template acetylsalicylic acid (aspirin) adsorbed on the p-ATP monolayer through hydrogen bonding. A conductive layer formed by electropolymerizing additional p-ATP, HAuCl_4 , and the template, resulting in an imprinted polymer containing AuNPs. The material showed increased conductivity and sensitivity due to nanoparticles [82]. Lee et al. developed a sensor for α -synuclein, a marker for Parkinson's disease. As a template, they used a peptide epitope of the protein. The electropolymerized MIPs were doped with various concentrations of transition metal dichalcogenides. The addition of WS_2 increased current density and doubled the sensor response to the analyte [102].

2.2.3. Thiophene-, Phenol-, and Benzoic-Acid-Based Systems

Thiophene-based systems are also inherently conductive materials. Nevertheless, sometimes they are further combined with nanomaterials. Moreira et al. reported an elec-

trochemical sensor for fructose detection. The device is based on phenylboronic acid and graphene oxide (GO) [103]. Wang et al. used AuNPs capped with 3-thiophene acetic acid (3-TAA) and electropolymerized them onto an electrode to obtain an adenine-imprinted conductive polymer. This strategy resulted in a very homogeneous conductive material [104]. Liu et al. developed an electrochemical sensor for epinephrine, a derivative of a neurotransmitter in the mammalian central nervous system. For this task, they prepared a MIP/AuNP composite on a GC electrode. The sensor is able to sensitively and selectively detect the analyte. Both the conductive polymer matrix and the AuNPs enhance device sensitivity. Compared to other electrochemical sensors for this analyte, it covered a wider linear range and reached a lower LOD. It showed double recognition: first, because of the complementary shape of the imprints. Second, the boronic acid covalently interacts with the cis-diol of the template [105]. Lach et al. developed a sensor to detect p-synephrine. They simultaneously imprinted the template and covalently immobilized a ferrocene redox probe in a (bis-bithiophene)-based polymer. This resulted in a redox self-reporting MIP-film-based chemosensor that operates in solutions that do not contain redox probes [106]. Chen et al. presented an adrenaline sensor based on MIPs combined with MXene/carbon nanohorn composite, which reached lower LOD values than previously reported adrenaline sensors. Furthermore, the results were in good agreement with those from HPLC [107]. Lee et al. produced a conductive MIP for matrix metalloproteinase-1 on a continuous monolayer of molybdenum disulfide (MoS₂). They first prepared the MoS₂ layer via chemical vapor deposition and then electropolymerized peptide-imprinted poly(triphenylamine rhodanine-3-acetic acid-co-3,4-ethoxylene dioxy thiophene) on top [108].

Furthermore, polyaminobenzoic acid is a conductive polymer, but it has been used in nanocomposites. Sun et al. reported a three-dimensional electrochemical sensor for sulfamerazine, a broad-spectrum antibiotic. They first modified a GC electrode with amino-functionalized MWCNTs@covalent organic frameworks (NH₂-MWCNT@COF) and MoS₂ nanosheets. Then, they prepared a MIP membrane on the surface of the electrode by electropolymerizing para-aminobenzoic acid [109]. As a proof-of-concept for a sensor array for β -lactam antibiotics in milk, Moro et al. developed a sensor for cefquinome. It consists of an electropolymerized poly-aminobenzoic acid MIP coupled to MWCNTs. The monomer was selected using computational modelling [110].

Wang et al. demonstrated a glycoprotein sensor based on MIPs prepared by electropolymerizing o-phenylenediamine and 3-amino-phenylboronic acid monohydrate in the presence of BSA. Adding graphene–Au nanoparticle hybrids dramatically improved sensitivity. BSA sensing took place by detecting the electrochemical oxidation signal of 6-ferrocenylhexanthiol, which was immobilized on the nanoparticles as the electroactive species [111].

Not all electropolymerized matrices are automatically conductive. Polyphenol, for example, is non-conductive and requires additives when preparing cMIP. For instance, Martins et al. used 3-nitrotyrosine, a biomarker for oxidative stress, as the template together with phenol as the functional monomer. They introduced conductivity by using carbon ink [112]. Cai et al. vertically aligned CNTs on titanium-coated glass substrates. They embedded the nanotubes in photoresist and polished the material to expose the tips followed by electropolymerization of polyphenol on CNT tips via CV. The CNTs give the material its conductivity. The LOD obtained for human ferritin surpasses the values obtained using conventional MIP sensors and is comparable results from to nanosensors with biomolecular recognition [80]. Table 2 gives an overview of the different systems described based on cMIPs with additives.

Table 2. Overview of cMIP sensors prepared using electropolymerization-including additives. All LOD values were converted into mol/L (if possible) to allow better comparison. DPV = differential pulse voltammetry, EIS = electrochemical impedance spectroscopy, SWV = square wave voltammetry, CV = cyclic voltammetry, LSV = linear sweep voltammetry.

Monomer	Additive	Analyte	Transducer	LOD [mol/L]	Ref.
Pyrrole	CS ₂ -functionalized GO	Cadmium	DPV	2×10^{-9}	[77]
Pyrrole	Dopamine@graphene	Olaquinox	DPV	7.5×10^{-9}	[78]
Pyrrole	MWCNT/GAs	Dopamine	DPV	1.67×10^{-9}	[79]
Pyrrole	MXene/NH ₂ -CNTs	Fisetin	DPV	1.0×10^{-9}	[81]
Pyrrole	Prussian-Blue-porous carbon-CNT hybrids	Cysteine	DPV	6×10^{-15}	[85]
Pyrrole	Au-NPs	Caffeine	DPV	0.9×10^{-9}	[86]
Pyrrole	Coomassie BB	Ricin (chain A)	EIS	3.13×10^{-12}	[87]
Pyrrole	Copper oxide	Tyrosine	DPV	4.0×10^{-9}	[88]
Cysteine	Biochar	Pb ²⁺ , Cd ²⁺	Differential pulse anodic stripping voltammetry	5.86×10^{-15} (Pb ²⁺) 0.883×10^{-18} (Cd ²⁺)	[89]
Aniline	Copper nanoparticles	Nitrate	LSV, EIS	31×10^{-6} (EIS) 5×10^{-6} (LSV)	[83]
Aniline, metanilic acid	WS ₂	17β estradiol	CV	0.2×10^{-18}	[90]
Aniline	C-dots	L-ascorbic acid, D-ascorbic acid	DPV	0.00016×10^{-9} (D) 0.00073×10^{-9} (L)	[91]
Aniline, m-aminobenzenesulfonic acid	MXene (e.g., Ti ₂ C)	C-reactive protein	CV	1.67×10^{-21}	[92]
Aniline	PMB/MWCNTs	Cardiac troponin	DPV	1.7×10^{-15}	[93]
Aniline or 2-methoxyaniline	GO	Amoxicillin	SWV	2.6×10^{-6} 6.1×10^{-7}	[94]
Aminophenol	Carbon ink	Carcinoembryonic antigen	EIS	16.7×10^{-12}	[95]
Aminophenol	Perovskite quantum dots	Prometryn	Electroluminescence	0.2×10^{-6} $0.010 \mu\text{g}/\text{kg}$ (fish)	[96]
o-phenylenediamine	poly(p-aminobenzene sulfonic acid)	Paracetamol	DPV	4.3×10^{-8}	[97]
o-phenylenediamine	Au-NPs	Tetracycline	DPV	0.32×10^{-9}	[98]
o-phenylenediamine	UCNPs@ZIF-8	Imidacloprid	Electroluminescence	39.1×10^{-15}	[99]
o-phenylenediamine	MPA-Cu NCs	Enrofloxacin	Electroluminescence	27×10^{-12}	[100]
p-ATP	Au-NPs	Aspirin	DPV	0.3×10^{-9}	[82]
p-ATP	N,S co-doped GQDs, Au-NPs	Sofosbuvir	DPV	0.36×10^{-9}	[84]
p-ATP	Au-NPs	Chlorpyrifos	CV	0.33×10^{-6}	[101]
Aniline, m-aminobenzenesulfonic acid	WS ₂	α-synuclein	CV	0.04×10^{-15}	[102]
Phenylboronic acid	RGO	Fructose	DPV	3.2×10^{-15}	[103]
3-thiopheneacetic acid	Au-NPs	Adenine	DPV	0.99×10^{-9}	[104]
3-thiopheneboronic acid	Au NPs	Epinephrine	DPV	76×10^{-9}	[105]
2,2'-bithio-phene-5-carboxylic acid	bis-(2,2'-bithienyl)-4-ferrocenylphenyl methane	p-synephrine	DPV	0.57×10^{-9}	[106]
Hydroxymethyl-3,4-ethylenedioxythiophene	MXene/carbon nanohorn	Adrenaline	DPV	0.3×10^{-9}	[107]
Triphenylamine rhodanine-3-acetic acid, EDOT	MoS ₂	Matrix metalloproteinase-1	CV	18.52×10^{-18}	[108]
para-aminobenzoic acid	MoS ₂ /NH ₂ -MWCNT@COF	Sulfamerazine	DPV	0.11×10^{-6}	[109]

Table 2. Cont.

Monomer	Additive	Analyte	Transducer	LOD [mol/L]	Ref.
4-aminobenzoic acid	MWCNTs	Cefquinome	SWV	50×10^{-9} ^A	[110]
o-phenylenediamine, 3-aminophenylboronic acid monohydrate	graphene-Au NPs	BSA	Electrochem. oxidation of grafted 6-ferrocenyl- hexanthiol	0.1×10^{-12}	[111]
Phenol	carbon ink	3-nitrotyrosine Human ferritin,	DPV	22.3×10^{-9}	[112]
Phenol	CNTs	human papillomavirus derived E7 protein	DPV	$\sim 0.21 \times 10^{-18}$ (hFtn) $< 0.91 \times 10^{-18}$ (E7)	[80]

^A No LOD given. Lowest detectable concentration.

2.3. Oxidative Polymerization

It is also possible to form conductive polymers using chemical oxidative polymerization. This approach usually relies on ammonium persulfate as an oxidizing agent [113]. As can be seen from the few examples below (Table 3), this technique is far less common than electropolymerization for cMIP preparation. In the publications below, mainly PANI was prepared with this method. Oxidative polymerization can be useful for fabricating cMIPs on non-conductive materials, which is not possible using electropolymerization [114]. In this way, Chen et al. prepared low-cost paper glucose sensors relying on resistive detection [115]. Singh et al. used this method to develop sensors for the mycotoxins Aflatoxin B1 and Fumonisin B1 based on PANI synthesized via oxidative polymerization [116].

Table 3. Overview of cMIP sensors prepared using oxidative polymerization. All LOD values were converted into mol/L (if possible) to allow better comparison. DPV = differential pulse voltammetry, CV = cyclic voltammetry, OCP = open circuit potential.

Monomer	Analyte	Transducer	LOD [mol/L]	Ref.
Aniline	Glucose	Resistive	1.0048×10^{-3}	[115]
Aniline	Aflatoxin B1	DPV	1.00×10^{-12} (AFB1)	[116]
Aniline, metanilic acid	Fumonisin B1	DPV	44.61×10^{-12} (FuB1)	[116]
4,4'-methylenedianiline	Testosterone	CV	$\sim 3 \times 10^{-6}$	[117]
3-aminophenylboronic acid	1-benzothiophene	CV	67.06×10^{-6}	[118]
	N-(1-desoxy-β-D-fructopyranose-1-yl)-L-valine	OCP	10×10^{-3} ^A	[119]

^A No LOD given. Only this concentration measured.

Liu et al. used self-assembly of poly(aniline-co-metanilic acid) to fabricate testosterone MIPs. Co-polymerization with metanilic acid leads to the formation of self-doped PANI films. Compared to other testosterone detection methods, the linear range of this sensor is lower [117]. Self-crosslinked 4,4'-methylenedianiline was prepared by Mohseni et al. using chemical oxidative polymerization with ammonium persulfate. The polymer was imprinted with 1-benzothiophene, an organosulfur compound associated with the source of crude oil [118]. Chuang et al. prepared a MIP to detect the amadori compound N-(1-desoxy-β-D-fructopyranose-1-yl)-L-valine. They deposited the polymer on conductive ITO layers on glass substrates. Polymerization took place in aqueous solution of 3-aminophenylboronic acid and ammonium persulfate [119].

2.4. MIPs + Conductive Nanomaterials

Acrylic or vinylic monomers are a popular choice for conventional MIPs. However, the resulting polymers are usually not electrically conductive. Therefore, those kinds of MIPs are typically combined with gravimetric or optical transducers. To make them accessible to

electrochemical sensors, additives that increase conductivity of the material are necessary. In the literature, there are several examples for this.

2.4.1. Acrylic Acid Derivatives as Monomers

Methacrylic acid (MAA) is usually the monomer of choice in most applications. Different corresponding examples for gas and small-molecule MIPs can be found in the literature. For acetone, Jahangiri-Manesh et al. developed a chemiresistor based on a MIP/AuNP nanocomposite. The MAA/ethylene glycol dimethacrylate (EGDMA) MIP was prepared using precipitation polymerization [120]. The same group also developed a similar device for nonanal, a cancer biomarker. This sensor is suitable for detecting the analyte in the headspace of human serum without the need of preconcentration [121]. A cMIP chemiresistor for toluene was prepared by polymerizing MAA and divinylbenzene (DVB) in toluene to a monolith and using the ground material together with carbon black and melted n-eicosane. The paste was packed into a cylindrical chemiresistor for toluene detection. The resulting sensor led to higher selectivity toward the analyte compared to previously reported toluene MIP sensors [122]. In a similar approach, the same group immobilized ethanol-imprinted p-MAA particles together with MWCNTs in poly(methyl methacrylate) (PMMA) [123]. Additionally, they also demonstrated a cMIP chemiresistor device for nitrobenzene based on methacrylic acid/vinyl benzene MIP particles and graphene [124]. A chemiresistor for the detection of gaseous hexanal was developed by Janfaza et al. They prepared MAA/EGDMA MIP nanoparticles via precipitation polymerization and dispersed the particles in PMMA together with the MWCNTs to obtain resistive ink. The nanocomposite was drop-casted on interdigitated electrodes [125]. Halim et al. demonstrated a reduced graphene oxide (RGO)/MIP organic thin film transistor for L-serine. RGO was added to a mixture containing MAA, EGDMA, and the template. This mixture was pipetted onto the transistor and polymerized under UV light [126,127]. A sensor for tylosin was developed by Zhang et al. They combined the MIP with self-supported CoN nanowire arrays grown on carbon cloth [128]. Li et al. fabricated an electrochemical MIP sensor based on Fe₃O₄ nanobeads and AuNPs on RGO for detecting ractopamine in water. They prepared the polymer using reversible addition fragmentation chain transfer (RAFT) polymerization to avoid low capacity and poor binding-site accessibility. RAFT MIPs have higher affinities toward analytes and exhibit rather homogeneous structures and distribution of cavities. Compared to other electrochemical ractopamine sensors, this device performed better with a low linear range and LOD [129]. Beigmoradi et al. modified a graphite-epoxy electrode with a Cu-metal-organic framework (Cu-MOF) and MIP. The MAA/EGDMA polymer was imprinted with carbendazim. The performance of the resulting sensor was comparable to other electrochemical methods for carbendazim detection as well as HPLC [130]. Ge et al. prepared a sensor array to detect acidic gases (propanoic acid, hexanoic acid, heptanoic acid, and octanoic acid). The polyacrylic acid MIP was placed on top of a conductive carbon black ink layer. Acetic acid was used as a template for imprinting the acid functional group [131]. A chemiresistor based on conductive polyacrylic acid ink containing carbon black particles was developed by Shinohara et al. They used it to detect hexanoic acid vapor in air [132]. An overview of MAA based cMIP sensors and other conductive nanomaterials is given in Table 4.

2.4.2. Aliphatic/Non-Aromatic Monomers

Prasad et al. developed a MIP for BSA detection on a MWCNT-modified ceramic electrode. This sensitive layer made ultra-trace detection of the protein possible in real samples, such as serum and milk [133]. For insulin, a sensor consisting of a gold electrode modified with carboxylated MWCNTs and MIP cryogel has been reported. The CNTs increase both surface area and conductivity of the material and reduce the required potential to oxidize insulin. At the same time, the cryogel MIP provides selective recognition of the analyte. Measurements in human serum samples using SWV gave similar results as a commercial electrochemiluminescence immunoassay [134]. Shao et al. developed a sensor consisting of

MIP on a GC electrode modified with AuNPs and MXene for tetrabromobisphenol A detection. They first prepared the modified electrode and immobilized the RAFT agent, followed by preparing the MIP (4-vinyl pyridine/EGDMA) by RAFT polymerization [135]. Wu et al. developed a tryptophan sensor based on imprinted chitosan films on MWCNT-modified electrodes [136].

Table 4. Overview of cMIP sensors with non-conductive MIPs and conductive nanomaterials. LOD values for gaseous analytes are given in ppm. All other LOD values were converted into mol/L to allow better comparison. The upper part of the table presents only sensors for gaseous analytes, the lower part applications in solution. DPV = differential pulse voltammetry, SWV = square wave voltammetry.

Monomer	Additive	Analyte	Transducer	LOD [ppm]	Ref.
MAA	AuNPs	Acetone	Resistive	66	[120]
MAA	AuNPs	Nonanal	Resistive	4.5	[121]
MAA	Carbon black	Toluene	Resistive	0.8	[122]
MAA	MWCNTs	Ethanol	Resistive	0.5	[123]
MAA, vinyl benzene	Graphene	Nitrobenzene	Resistive	0.2	[124]
MAA	MWCNTs	Hexanal	Resistive	10	[125]
Polyacrylic acid	Carbon black	Acid gases ^A	Resistive	–	[131]
Polyacrylic acid	Carbon black	Hexanoic acid	Resistive	100 ^B	[132]
Monomer	Additive	Analyte	Transducer	LOD [mol/L]	Ref.
MAA	GO	L-serine	Thin film transistor	0.19×10^{-3}	[126,127]
MAA	CoN nanowires	Tylosin	DPV	5.5×10^{-12}	[128]
MAA	Au@Fe ₃ O ₄ @RGO-MIPs	Ractopamine	DPV	0.02×10^{-9}	[129]
MAA	Cu-MOF	Carbendazim	DPV	2×10^{-9}	[130]
Tetraethylene Glycol 3-morpholin propionate acrylate	MWCNTs	BSA	DPV	0.36×10^{-9}	[133]
Acrylamide (AA)	MWCNTs	Insulin	SWV	33×10^{-15}	[134]
4-vinyl pyridine	MXene, AuNPs	Tetrabromobisphenol A (TBBPA)	DPV	14.4×10^{-12}	[135]
Chitosan	MWCNTs	Tryptophan	Second-order derivative linear sweep voltammetry	1.0×10^{-9}	[136]
Polyvinylphenol	SWCNTs	Cotinine	Resistive	0.28×10^{-6}	[137]
Sodium p-styrenesulfonate, dopamine	MWCNTs, AgNPs	Sulfonamides	DPV	4×10^{-9}	[138]

^A Propanoic acid, hexanoic acid, heptanoic acid, and octanoic acid. ^B No LOD. Only this concentration measured.

2.4.3. Aromatic Monomers

Antwi-Boampong et al. presented a molecularly imprinted polyvinylphenol composite with single walled carbon nanotubes (SWCNTs). This sensor was developed for detecting cotinine, a metabolite of nicotine. Polyvinylphenol was dissolved in methanol together with CNTs and the template, followed by spin coating onto the sensor [137]. Han et al. improved both sensitivity and selectivity of a sulfonamide sensor by introducing polydopamine to the MIP. They polymerized dopamine together with the functional monomer sodium p-styrenesulfonate and the cross-linker EGDMA in the presence of the template sulfamethoxazole. This improved selectivity as well as conductivity compared to MIPs without dopamine. The precipitated MIPs were mixed with graphite powder, and MWCNT-silver nanoparticles (AgNPs), homogenized with liquid paraffin and packed into a carbon paste electrode. The sensor performed well in food samples, and the LOD exceeded previously reported values [138].

2.5. Blending MIPs with Conductive Polymers

Another way to introduce conductivity into MIP-based sensing layers is the combination of conventional, non-conductive MIPs with non-imprinted (semi)conductive polymers (Table 5). Lee et al., for instance, reported a chemiresistor array for the detection of various terpenes. They used polymethacrylic acid imprinted with either α -pinene, limonene, linalool, or geraniol and introduced the conductivity necessary for resistive measurements by blending the MIPs with PANI [139]. Similarly, Völkle et al. prepared polymer blends of imprinted polystyrene-co-DVB and the semiconductive poly(3-hexylthiophene) (P3HT). The resulting polymer blend was successfully applied on QCM and chemiresistor sensors for detecting limonene in gaseous phase [140]. While embedding non-conductive MIPs into an organic semiconductor matrix represents a very straightforward way to introduce conductivity into sensing layers, one must ensure that binding site accessibility is not compromised by the blending process. This can be addressed by the formation of nanocomposites, which display a high surface area and thus a large number of accessible binding sites. For instance, Koudehi et al. reported sensing layers based on a blend of PPy nanoparticles and imprinted polyvinyl alcohol (PVA) nanoparticles for the detection of the explosive 2,4-dinitrotoluene (2,4-DNT). The PVA/PPy/MIP nanocomposites displayed good flexibility and adhesiveness due to the PVA, as well as high selectivity and fast response times in resistive measurements [141].

Table 5. Overview of cMIP sensors with polymer blends. LOD values for gaseous analytes are given in ppm. All other LOD values were converted into mol/L to allow better comparison. QCM = quartz crystal microbalance, DPV = differential pulse voltammetry.

Monomer	Cond. Polymer	Analyte	Transducer	LOD [ppm]	Ref.
MAA	PANI	Terpenes ^A	Resistive	~50 ^B	[139]
Styrene	P3HT	Limonene	QCM	50 ^B	[140]
PVA	PPy	2,4-DNT	Resistive	0.1	[141]
Monomer	Additive	Analyte	Transducer	LOD [mol/L]	Ref.
AA	FUN-PANI	Parathion	DPV	1.13×10^{-8}	[142]
AA	MWCNT/PANI	Nalbuphine	Potentiometric	1.1×10^{-7}	[143]

^A α -Pinene, limonene, linalool, and geraniol; ^B lowest measured concentration.

Similarly, Liang et al. used PANI nanoparticles functionalized with vinyl groups (FUN-PANI). They polymerized an AA/EGDMA-based MIP in the presence of the analyte parathion onto the particles' surface. This ensured the presence of accessible binding sites at the surface, while also introducing the desired electrochemical properties into the sensing material. The resulting FUN-PANI-MIP films allowed for fast and selective voltametric detection of the analyte, which was in good agreement with results obtained by HPLC [142].

The performance of sensing layers composed of conventional MIPs and organic semiconductors can be further enhanced by forming more complex multi-component blends. For instance, Hassan et al. synthesized nalbuphine-imprinted AA/EGDMA particles using precipitation polymerization. For potentiometric detection, the particles were incorporated in a PVC membrane together with a nanocomposite consisting of functionalized MWCNTs and PANI. The composite material maintained its selective properties, while displaying a significantly improved potential stability and durability, owing to the modification with the MWCNT/PANI nanocomposite layer [143].

3. Applications in Chemical Sensing

3.1. Transducers

Conventional (non-conductive) MIPs are often combined with mass-sensitive transducers. Those devices rely on the piezoelectric effect and react to adsorbed mass with a change in frequency. The most frequently used piezoelectric transducer is the quartz crystal

microbalance (QCM), which is also useful with cMIPs [27,112,114,116]. SAW resonators represent a different kind of piezoelectric sensor, which can be combined with cMIPs [65]. However, those transducers do not require electrically conductive polymers. cMIPs reveal their full potential when combining them with electrochemical transducers: electrically conductive polymers or composites enable electron transfer to the electrodes (Figure 5). However, they are not only useful to detect electroactive analytes. In that case, it is necessary to add an electroactive probe (sometimes referred to as “electrochemical indicator”) to the sample.

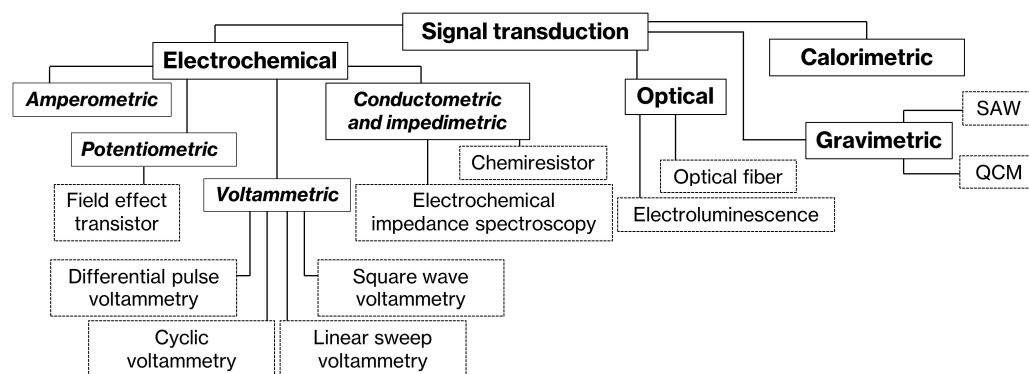


Figure 5. Signal transduction possibilities for cMIP-based sensing layers. Adapted from [144,145].

Voltammetric methods are very selective since they identify the analyte via specific oxidation and reduction peaks [24]. Popular detection methods include DPV (e.g., [35,45,60]) and CV (e.g., [54,90,108]). Other examples utilize square wave voltammetry [40,94,110,134] or linear sweep voltammetry [83]. Amperometric sensors comprising cMIPs [33,34,38,39] are less common. Those devices are a subgroup of voltammetric methods in the sense that they operate at a fixed potential. The analyte binds to the imprints and becomes reduced or oxidized, which, in turn, generates a current proportional to analyte concentration [12]. There are also a few examples of potentiometric detection [119,143], electric impedance spectroscopy (e.g., [37,59,62]), and resistive devices [120–125,131,132]. EIS devices measure the impedance of the system. They are sensitive to capacitive and inductive effects [12]. In resistive sensors, the binding event causes a change in electric resistance, or in other words, conductivity, of the receptor material. Such sensor types mainly rely on composites consisting of (acrylic) MIPs and conductive nanomaterials. Adsorption of the analyte causes swelling of the polymer film, which means that the conductive parts of the material move further apart. Those devices are usually not suitable for measuring in buffers due to the high ionic strength of the medium. Therefore, they are mainly used for gas sensing applications [146]. Other, less common transducers mentioned in this review include thermal resistance measurements [42], optical fiber [43,44], EG-FET [66], thin film transistor [126,127], and electroluminescence [96,99,100].

3.2. Application Areas

Although cMIP-based sensing systems are potentially useful for a wide range of applications, most reports focus on food safety, medical applications, and environmental monitoring. Within these areas, sensors have been developed for all sizes of analytes ranging from heavy metals, to pharmaceuticals and proteins, to microbiological systems. This section therefore aims to provide a short overview of current sensing systems. A graphical summary for all applications is depicted in Figure 6.

3.2.1. Food Safety

Sulfadimethoxine is a sulfonamide antibiotic that is used in animal husbandry for food products of animal origin that may contain residues of the compound and, thus, cause adverse health effects for the consumer. To detect sulfadimethoxine, a sensing system based on electropolymerized PPy was reported [33] and further optimized, which lowered

the LOD [34] (Table 1). Doxycyclin is a similar antibiotic: it is also used in veterinary medicine and aquaculture. Residues can be found in food products, such as meat, eggs, and milk, and can be detected with a cMIP-based sensor, developed by Gürler et al. [32] (Table 1). Other sensors for antibiotics in food include sulfonamide detection in chicken, pork, and egg [138] (Table 4) as well as detecting tetracycline antibiotic residues in milk and meat [98] (Table 2). As an example, for animal growth promoters, a sensing system for olaquinox was developed. Olaquinox contamination in food products and water sources may negatively affect humans, animals, and the environment. The sensor relies on imprinted PPy on dopamine@graphene. It is able to measure contamination in spiked fish and feedstuff [78] (Table 2). Melamine has been used as a fake protein source in infant formula and pet food in China. It is connected to acute renal failure in animals and humans due to kidney stone formation. Regasa et al. prepared a sensor for this compound and successfully analyzed melamine in spiked infant formula and raw milk [56] (Table 1).

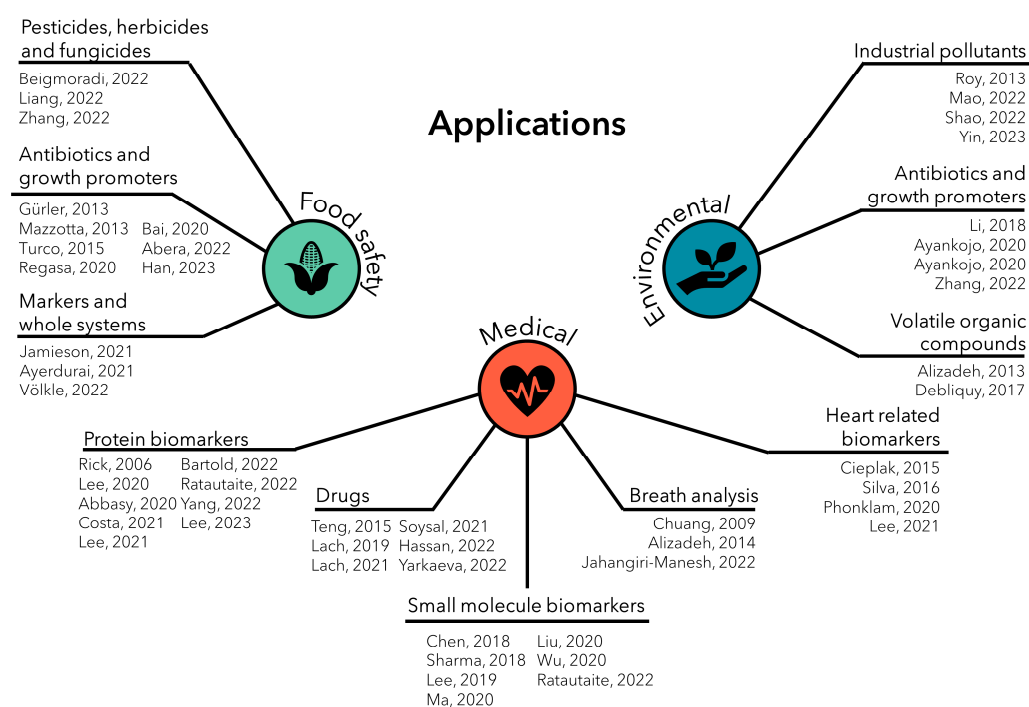


Figure 6. General overview of the different application areas of cMIP-based sensors, cited from [32–35,37,39,40,42,43,45,47,48,54–56,58,63,66,67,76–78,88,91–93,95–97,101,105,107,116,119,120,122,124,127–129,134,135,137,139,140].

Organophosphate pesticides are widely used to limit infestations on agricultural products. Liang et al. prepared a sensor for parathion by imprinting the pesticide on functionalized PANI nanoparticles, which made it possible to detect it in vegetable samples [142] (Table 5). Prometryn is a triazine herbicide commonly used for controlling weeds and algae in aquaculture. However, the compound is rather stable, accumulates in aquatic products, and is potentially harmful for human health and the environment. Zhang et al. developed a MIP sensor comprising quantum dots to detect prometryn in fish and water samples [96] (Table 2). Carbendazim is a fungicide frequently used in agriculture. It is suspected to cause cancer. Beigamoradi et al. developed a sensor for this substance and tested it in various food samples, including tangerine, tomato, apple, and cucumber [130] (Table 4).

Tyramine is a well-known marker for rottenness; a sensor to detect it in different food samples was successfully established [60] (Table 1). Terpenes such as limonene constitute another relevant marker for degradation of organic matter. It is possible to detect them in the gas phase with a cMIP sensor [140] (Table 5). Besides markers and contaminations, whole cell systems such as yeast, which are relevant to food, can be monitored using heat transfer detection with electropolymerized MIPs [42] (Table 1).

3.2.2. Medical Applications

Sensors based on cMIPs are often used to detect protein biomarkers in different media. This starts with heart-related markers, such as HSA, which can be monitored in serum to prevent liver and heart diseases [37] (Table 1). Cardiac troponin T is another important example: it helps to diagnose and treat myocardial infarction [45] (Table 1). Another troponin T sensor achieved results in diluted human blood plasma that agree well with those of the gold standard, electrochemiluminescence immunoassay [93] (Table 2). C-reactive protein is another marker for coronary heart disease, inflammatory diseases, and viral infections, for which a cMIP-based sensor for detection in serum was developed [92] (Table 2).

Besides heart related markers, other important protein biomarkers were successfully used to prepare cMIP-based sensors. A prominent example is a sensor based on imprinted epitopes of matrix metalloproteinase-1 (MMP-1). The latter is an idiopathic IPF marker and not yet fully understood, making the sensor a valuable tool [66] (Table 1). A second sensor for the same analyte was developed by Lee et al. by electropolymerizing a peptide-imprinted polymer. The resulting sensor demonstrated good results compared to ELISA in A549 cell line culture medium [108] (Table 2). Lee et al. developed a sensor for α -synuclein, which is a marker for Parkinson's disease. It was successfully applied in SNCA in culture medium of midbrain organoids [58,102] (Tables 1 and 2). PSA levels are associated with prostate cancer; a corresponding sensor for detecting it in human serum exists in the literature [67] (Table 1). Lysozyme is found in body fluids, and unusual levels may indicate pathological conditions, which was the reason for developing different sensors for Lysozyme [48,61] and cytochrome c [48] (Table 1). As an example for addressing viral markers, Ratautaite et al. developed a sensor for the SARS-CoV-2 spike glycoprotein, which has been of crucial importance since the beginning of the coronavirus pandemic [39] (Table 1). Although Cor a 14 allergen is an allergen and not directly a biomarker, it has to be mentioned here, since the respective sensor remarkably demonstrated a higher selectivity of the MIP compared to Cor than a 14 IgG produced in rabbits [40] (Table 1).

Aside from large protein-based markers, one can find a similar number of applications to detect small-molecule biomarkers. Examples thereof are sensors for L-tryptophan [35,136] (Tables 1 and 4), testosterone [117] (Table 3), oxytocin nonapeptide [62] (Table 1), or multichannel monitoring of the hormones 17β estradiol, cortisol, progesterone, and testosterone [54] (Table 1). Additionally, devices to detect dopamine have been developed. High levels of dopamine can cause ADHD and schizophrenia in children, whereas low levels lead to Parkinson's and Alzheimer's disease in elderly people [47,79] (Tables 1 and 2).

Furthermore, one can find some applications regarding drugs. Sensors were also developed for p-synephrine, a dietary supplement for weight loss, which comes with serious side effects such as high blood pressure, myocardial infarction, and sudden death [59,106] (Tables 1 and 2). Nalbuphine hydrochloride is a phenanthrene derivative of opioid analgesics and is used for treating pain. It comes with a range of side effects, such as nausea, dehydration, and dizziness. A sensor to monitor the compound in pharmaceutical drugs and spiked urine samples was established [143] (Table 4). In addition, examples for cMIP sensors for well-known drugs include an example each for the antibiotic amoxicillin [94] and the painkiller paracetamol [97] (Table 2). Not only drugs, but also other health relevant molecules, such as endocrine disrupting compounds, can be assessed. For example, 4-hydroxybenzoic acid esters, which are frequently used as antimicrobial additives in cosmetics and pharmaceutical products, were successfully measured in real samples with a novel sensor [63] (Table 1).

In addition to the mentioned applications, cMIPs potentially play a crucial role in future breath analysis. Breath analysis is an attractive alternative to invasive diagnosis, and it has already led to the development of some sensors for breath biomarkers. These include acetone, which is present in the exhaled air of diabetes patients [119], and nonanal [120] and hexanal [124], which are both breath biomarkers for lung cancer (Table 4).

3.2.3. Environmental Applications

A wide range of environmental pollutants are known; monitoring them becomes an increasingly important issue due to the strong worldwide population increase. For instance, heavy metal pollution from industrial processes may contaminate food or water and affect human health [77]. Pb^{2+} and Cd^{2+} sensors with nanobiochar and electropolymerized L-cysteine were developed to enable monitoring of such pollutants in real-life water samples. The sensor reached LODs considerably lower than the minimum detection concentrations specified by WHO [89] (Table 2).

Ractopamine is a β -androgenic leanness-enhancing agent usually fed to bred animals to boost muscle tissue growth; it can cause harm to human health by influencing the cardiovascular and central nervous system. For monitoring the compound, a cMIP sensor based on $Au@Fe_3O_4@RGO$ -MIPs was developed [129] (Table 4). Para-nitrophenol is a toxic pesticide that pollutes soil and wastewater. It is known to have carcinogenic and mutagenic effects. Roy et al. prepared a sensor for this compound [55] (Table 1). Tetrabromobisphenol A is a flame retardant often used in industrial manufacturing. It tends to accumulate in water and poses risks for the environment and human health. Shao et al. developed a suitable cMIP sensor that can detect the substance in water samples [135] (Table 3).

Besides direct environmental contamination by toxic compounds, bacterial resistance to antibiotics is a growing and crucial challenge, which requires monitoring antibiotic levels in water. For this purpose, cMIP-based sensors to detect erythromycin in tap water [64] (Table 1) and tylosin in real surface water and soil samples were developed [128] (Table 4). Another example is a sensor for sulfamethizole, which was developed by the same group [65] (Table 1).

In terms of indoor contaminations, volatile organic compounds (VOCs) are an issue of growing concern. Additionally for this application, cMIP-based sensing systems such as a formaldehyde [43] (Table 1) or toluene sensors [122] (Table 4) are valuable to extend the application range toward more VOCs.

4. Summary and Discussion

The most widespread monomers used for molecular imprinting, such as acrylic or vinylic compounds, result in electrically insulating polymers. This limits the applications of the materials in chemical sensing. Methods that require direct conduction of electrons between the binding sites or direct monitoring of electrical changes in the receptor film cannot be integrated with conventional MIPs. cMIPs fill this gap as they combine the advantages of both methods: the imprints in the material provide selective recognition of the analyte, and the conductive polymer and/or additive allows for integrating them into a wider range of transducers. Combining MIPs with conductive additives often also enhances affinity and sensitivity of the sensors by increasing surface area or conductivity.

As can be seen in the examples above, cMIP sensors have already been developed for a wide range of analytes. These include ions, simple gas molecules, and drugs, as well as larger species, such as proteins and cells, and they are not limited to a single sensing strategy. Depending on the desired product and application, one can choose between electropolymerizing suitable monomers or preparing conventional MIPs with conductive additives. So far, electropolymerization is more widespread for cMIP fabrication. In particular, electropolymerization of pyrrole with and without additives has been performed for a variety of analytes. Electropolymerization has the advantage of forming uniform films whose thickness one can easily control. This is beneficial for good reproducibility among the sensors. Additionally, electropolymers—in contrast to other polymers—are often synthesized in aqueous solution, which is a better environment for biomolecules than organic solvents. The main drawback of electropolymerization is the limited number of suitable monomers and their lack of functionalities. This can be solved by synthesizing new, tailored monomers for future applications. An alternative approach is to combine non-conductive MIPs with conductive materials, since acrylic monomers present a larger variety of functionalities. Although this seems straightforward, several crucial issues need

considering, such as the sensitivity of the blending material toward the analyte or the measurement matrix, miscibility of the components, and degradation.

Generally, bulk MIPs may be limited in the sense that they lead to weak signals due to impeded diffusion to the binding sites or low number of binding sites. Those problems can be solved by increasing porosity or incorporating nanomaterials that enhance the active surface area. So far, cMIP sensors are, to the best of our knowledge, not used in commercial devices. As of now, most reported systems achieve highly promising results in controlled laboratory conditions. However, in order to move cMIPs toward commercial implementation, a thorough assessment of their performance in real-life samples and complex matrices is a necessary next step. Given that the field is relatively young and rapidly developing, cMIPs bear a huge potential for future applications. [147] Based on remarkable progress on the hardware side within the last 10 years, e.g., the widespread use of smartphone apps or the possibility for large-scale data monitoring (10–100 km radius) using open access networks, which neither requires a phone or service contract [148], a strongly increasing demand for accurate and stable sensors can be expected. This could be solved by, e.g., Universal Serial Bus (USB, or USB C)-based sensing platforms, which can be easily coupled with the digital world [75]. Simple sensing concepts, such as, e.g., chemiresistors in combination with cMIPs, therefore bear a huge potential to be tailored for a wide range of practical applications based on their sensing layer. The most important upcoming issue therefore will be to develop or identify systems that are stable and reliable for prolonged periods. This is often only a side aspect in publications, but the described cMIPs with the different fabrication and modification possibilities are a highly promising toolbox to close this gap.

This review aims to provide an overview about already established cMIP sensing systems and their application. Starting from electropolymerization as a classical technique to newer systems with a higher degree of complexity, the available literature clearly points out the versatility of conductive MIP systems in sensing. Based on the simplicity and applicability of cMIPs together with the limited number of publications in this field, one can safely assume strongly growing interest in the field.

Author Contributions: Conceptualization, A.F. and P.F.; writing—original draft preparation, A.F.; writing—review and editing, A.F., J.V., P.L. and P.F.; visualization, A.F. and J.V. All authors have read and agreed to the published version of the manuscript.

Funding: The authors gratefully acknowledge the Gesellschaft für Forschungsförderung Niederösterreich m.b.H. for funding the practical work related to this manuscript under grant number LSC19-013 and SC19-020 and the Österreichische Forschungsförderungs GmbH (FFG) for funding the Centre of Electrochemical Surface Technology within the COMET program (grant-No.: 865864).

Institutional Review Board Statement: Not applicable.

Informed Consent Statement: Not applicable.

Data Availability Statement: Not applicable.

Conflicts of Interest: The authors declare no conflict of interest. The funders had no role in the design of the study; in the collection, analyses, or interpretation of data; in the writing of the manuscript; or in the decision to publish the results.

References

1. Wulff, G. Forty years of molecular imprinting in synthetic polymers: Origin, features and perspectives. *Microchim. Acta* **2013**, *180*, 1359–1370. [[CrossRef](#)]
2. Haupt, K.; Medina Rangel, P.X.; Bui, B.T.S. Molecularly Imprinted Polymers: Antibody Mimics for Bioimaging and Therapy. *Chem. Rev.* **2020**, *120*, 9554–9582. [[CrossRef](#)] [[PubMed](#)]
3. Sullivan, M.V.; Allabush, F.; Bunka, D.; Tolley, A.; Mendes, P.M.; Tucker, J.H.R.; Turner, N.W. Hybrid aptamer-molecularly imprinted polymer (AptaMIP) nanoparticles selective for the antibiotic moxifloxacin. *Polym. Chem.* **2021**, *12*, 4394–4405. [[CrossRef](#)]
4. Khan, M.A.R.; Aires Cardoso, A.R.; Sales, M.G.F.; Merino, S.; Tomás, J.M.; Rius, F.X.; Riu, J. Artificial receptors for the electrochemical detection of bacterial flagellar filaments from *Proteus mirabilis*. *Sens. Actuators B Chem.* **2017**, *244*, 732–741. [[CrossRef](#)]

5. Kadhém, A.J.; Gentile, G.J.; de Cortalezzi, M.M.F. Molecularly Imprinted Polymers (Mips) in Sensors for Environmental and Biomedical Applications: A Review. *Molecules* **2021**, *26*, 6233. [[CrossRef](#)]
6. Canfarotta, F.; Poma, A.; Guerreiro, A.; Piletsky, S. Solid-phase synthesis of molecularly imprinted nanoparticles. *Nat. Protoc.* **2016**, *11*, 443–455. [[CrossRef](#)]
7. Wackerlig, J.; Lieberzeit, P.A. Molecularly Imprinted Polymer Nanoparticles in Chemical Sensing—Synthesis, Characterization and Application. *Sens. Actuators B Chem.* **2015**, *207*, 144–157. [[CrossRef](#)]
8. Herrera-Chacón, A.; Cetó, X.; del Valle, M. Molecularly imprinted polymers—Towards electrochemical sensors and electronic tongues. *Anal. Bioanal. Chem.* **2021**, *413*, 6117–6140. [[CrossRef](#)]
9. Han, Y.; Tao, J.; Ali, N.; Khan, A.; Malik, S.; Khan, H.; Yu, C.; Yang, Y.; Bilal, M.; Mohamed, A.A. Molecularly imprinted polymers as the epitome of excellence in multiple fields. *Eur. Polym. J.* **2022**, *179*, 111582. [[CrossRef](#)]
10. Xu, S.; Wang, L.; Liu, Z. Molecularly Imprinted Polymer Nanoparticles: An Emerging Versatile Platform for Cancer Therapy. *Angew. Chem. Int. Ed.* **2021**, *60*, 3858–3869. [[CrossRef](#)]
11. Hulanicki, A.; Glab, S.; Ingman, F. Chemical sensors: Definitions and classification. *Pure Appl. Chem.* **1991**, *63*, 1247–1250. [[CrossRef](#)]
12. Lowdon, J.W.; Diliën, H.; Singla, P.; Peeters, M.; Cleij, T.J.; van Grinsven, B.; Eersels, K. MIPs for commercial application in low-cost sensors and assays—An overview of the current status quo. *Sens. Actuators B Chem.* **2020**, *325*, 128973. [[CrossRef](#)] [[PubMed](#)]
13. Polyakov, M.V.; Kuleshina, L.; Neimark, I. On the Dependence of Silica Gel Adsorption Properties on the Character of Its Porosity. *Zhurnal Fizicheskoi Khimii/Akad. SSSR* **1937**, *10*, 100–112.
14. Dickey, F.H. The Preparation of Specific Adsorbents. *Proc. Natl. Acad. Sci. USA* **1949**, *35*, 227–229. [[CrossRef](#)] [[PubMed](#)]
15. Sajini, T.; Mathew, B. A brief overview of molecularly imprinted polymers: Highlighting computational design, nano and photo-responsive imprinting. *Talanta Open* **2021**, *4*, 100072. [[CrossRef](#)]
16. Bolto, B.A.; Weiss, D. Electronic Conduction in Polymers. II. The Electrochemical Reduction of Polypyrrole at Controlled Potential. *Aust. J. Chem.* **1963**, *16*, 1076–1089. [[CrossRef](#)]
17. Shirakawa, H.; Louis, E.J.; MacDiarmid, A.G.; Chiang, C.K.; Heeger, A.J. Synthesis of electrically conducting organic polymers: Halogen derivatives of polyacetylene, (CH)_x. *J. Chem. Soc. Chem. Commun.* **1977**, *16*, 578–580. [[CrossRef](#)]
18. Rasmussen, S.C. Early History of Polypyrrole: The First Conducting Organic Polymer. *Bull. Hist. Chem.* **2015**, *40*, 45–55.
19. Gangopadhyay, R.; De, A. Conducting Polymer Nanocomposites: A Brief Overview. *Chem. Mater.* **2000**, *12*, 608–622. [[CrossRef](#)]
20. Schadler, L.S.; Brinson, L.C.; Sawyer, W.G. Polymer nanocomposites: A small part of the story. *JOM* **2007**, *59*, 53–60. [[CrossRef](#)]
21. BelBruno, J.J. Molecularly Imprinted Polymers. *Chem. Rev.* **2019**, *119*, 94–119. [[CrossRef](#)]
22. Villa, C.C.; Sánchez, L.T.; Valencia, G.A.; Ahmed, S.; Gutiérrez, T.J. Molecularly imprinted polymers for food applications: A review. *Trends Food Sci. Technol.* **2021**, *111*, 642–669. [[CrossRef](#)]
23. Fresco-Cala, B.; Batista, A.D.; Cárdenas, S. Molecularly Imprinted Polymer Micro- and Nano-Particles: A Review. *Molecules* **2020**, *25*, 4740. [[CrossRef](#)]
24. Leibl, N.; Haupt, K.; Gonzato, C.; Duma, L. Molecularly Imprinted Polymers for Chemical Sensing: A Tutorial Review. *Chemosensors* **2021**, *9*, 123. [[CrossRef](#)]
25. Turiel, E.; Martín-Esteban, A. Molecularly imprinted polymers for sample preparation: A review. *Anal. Chim. Acta* **2010**, *668*, 87–99. [[CrossRef](#)]
26. Nezakati, T.; Seifalian, A.; Tan, A.; Seifalian, A.M. Conductive Polymers: Opportunities and Challenges in Biomedical Applications. *Chem. Rev.* **2018**, *118*, 6766–6843. [[CrossRef](#)] [[PubMed](#)]
27. Anantha-Iyengar, G.; Shanmugasundaram, K.; Nallal, M.; Lee, K.-P.; Whitcombe, M.J.; Lakshmi, D.; Sai-Anand, G. Functionalized conjugated polymers for sensing and molecular imprinting applications. *Prog. Polym. Sci.* **2019**, *88*, 1–129. [[CrossRef](#)]
28. Blanco-López, M.C.; Gutiérrez-Fernández, S.; Lobo-Castañón, M.J.; Miranda-Ordieres, A.J.; Tuñón-Blanco, P. Electrochemical sensing with electrodes modified with molecularly imprinted polymer films. *Anal. Bioanal. Chem.* **2004**, *378*, 1922–1928. [[CrossRef](#)] [[PubMed](#)]
29. Fuchiwaki, Y.; Kubo, I. Electrochemical Sensor Based on Biomimetic Recognition Utilizing Molecularly Imprinted Polymer Receptor. In *Biomimetics Learning from Nature*; Vellore Institute of Technology University: Vellore, India, 2010. [[CrossRef](#)]
30. Cowen, T.; Cheffena, M. Template Imprinting Versus Porogen Imprinting of Small Molecules: A Review of Molecularly Imprinted Polymers in Gas Sensing. *Int. J. Mol. Sci.* **2022**, *23*, 9642. [[CrossRef](#)]
31. Sharma, P.S.; Pietrzyk-Le, A.; D'souza, F.; Kutner, W. Electrochemically synthesized polymers in molecular imprinting for chemical sensing. *Anal. Bioanal. Chem.* **2012**, *402*, 3177–3204. [[CrossRef](#)]
32. Gürlér, B.; Özkörücü, S.P.; Kır, E. Voltammetric behavior and determination of doxycycline in pharmaceuticals at molecularly imprinted and non-imprinted overoxidized polypyrrole electrodes. *J. Pharm. Biomed. Anal.* **2013**, *84*, 263–268. [[CrossRef](#)] [[PubMed](#)]
33. Mazzotta, E.; Malitesta, C.; Surdo, S.; Barillaro, G. Microstructuring conducting polymers and molecularly imprinted polymers by light-activated electropolymerization on micromachined silicon. Applications in electrochemical sensing. In Proceedings of the SENSORS, 2013 IEEE, Baltimore, MD, USA, 3–6 November 2013; pp. 1–4. [[CrossRef](#)]
34. Turco, A.; Corvaglia, S.; Mazzotta, E. Electrochemical sensor for sulfadimethoxine based on molecularly imprinted polypyrrole: Study of imprinting parameters. *Biosens. Bioelectron.* **2015**, *63*, 240–247. [[CrossRef](#)] [[PubMed](#)]

35. Ratautaite, V.; Brazys, E.; Ramanaviciene, A.; Ramanavicius, A. Electrochemical sensors based on l-tryptophan molecularly imprinted polypyrrole and polyaniline. *J. Electroanal. Chem.* **2022**, *917*, 116389. [[CrossRef](#)]
36. Choong, C.-L.; Milne, W.I. Dynamic modulation of detection window in conducting polymer based biosensors. *Biosens. Bioelectron.* **2010**, *25*, 2384–2388. [[CrossRef](#)]
37. Cieplak, M.; Szwabinska, K.; Sosnowska, M.; Chandra, B.K.C.; Borowicz, P.; Noworyta, K.; D'souza, F.; Kutner, W. Selective electrochemical sensing of human serum albumin by semi-covalent molecular imprinting. *Biosens. Bioelectron.* **2015**, *74*, 960–966. [[CrossRef](#)]
38. Ramanaviciene, A.; Ramanavicius, A. Molecularly imprinted polypyrrole-based synthetic receptor for direct detection of bovine leukemia virus glycoproteins. *Biosens. Bioelectron.* **2004**, *20*, 1076–1082. [[CrossRef](#)] [[PubMed](#)]
39. Ratautaite, V.; Boguzaitė, R.; Brazys, E.; Ramanaviciene, A.; Ciplys, E.; Juozapaitis, M.; Slibinskas, R.; Bechelany, M.; Ramanavicius, A. Molecularly imprinted polypyrrole based sensor for the detection of SARS-CoV-2 spike glycoprotein. *Electrochim. Acta* **2022**, *403*, 139581. [[CrossRef](#)]
40. Costa, R.; Costa, J.; Moreira, P.; Brandão, A.T.S.C.; Mafra, I.; Silva, A.F.; Pereira, C.M. Molecularly imprinted polymer as a synthetic antibody for the biorecognition of hazelnut Cor a 14-allergen. *Anal. Chim. Acta* **2021**, *1191*, 339310. [[CrossRef](#)]
41. Tokonami, S.; Nakadoi, Y.; Nakata, H.; Takami, S.; Kadoma, T.; Shiigi, H.; Nagaoka, T. Recognition of gram-negative and gram-positive bacteria with a functionalized conducting polymer film. *Res. Chem. Intermed.* **2014**, *40*, 2327–2335. [[CrossRef](#)]
42. Jamieson, O.; Betlem, K.; Mansouri, N.; Crapnell, R.D.; Vieira, F.S.; Hudson, A.; Banks, C.E.; Liauw, C.M.; Gruber, J.; Zubko, M.; et al. Electropolymerised molecularly imprinted polymers for the heat-transfer based detection of microorganisms: A proof-of-concept study using yeast. *Therm. Sci. Eng. Prog.* **2021**, *24*, 100956. [[CrossRef](#)]
43. Debliquy, M.; Lahem, D.; Tang, X.; Krumpmann, A.; Gonzalez Vila, A.; Raskin, J.-P.; Zhang, C. Molecularly Imprinted Polymers for VOC Sensing: Chemoresistive and Optical Sensors. In Proceedings of the 2017 4th International Conference on Machinery, Materials and Computer (MACMC 2017), Xi'an, China, 27–29 November 2017; p. 7.
44. González-Vila, A.; Debliquy, M.; Lahem, D.; Zhang, C.; Mégret, P.; Caucheteur, C. Molecularly imprinted electropolymerization on a metal-coated optical fiber for gas sensing applications. *Sens. Actuators B Chem.* **2017**, *244*, 1145–1151. [[CrossRef](#)]
45. Silva, B.V.; Rodríguez, B.A.; Sales, G.F.; Sotomayor, M.D.P.T.; Dutra, R.F. An ultrasensitive human cardiac troponin T graphene screen-printed electrode based on electropolymerized-molecularly imprinted conducting polymer. *Biosens. Bioelectron.* **2016**, *77*, 978–985. [[CrossRef](#)] [[PubMed](#)]
46. Kim, J.-M.; Lee, U.-H.; Chang, S.-M.; Park, J.Y. Gravimetric detection of theophylline on pore-structured molecularly imprinted conducting polymer. *Sens. Actuators B Chem.* **2014**, *200*, 25–30. [[CrossRef](#)]
47. Chen, L.; Liu, D.; Wang, C. A Novel Imprinted Electrochemical Sensor for Dopamine Determination Based on Electron Conductivity Enhanced by Ferrocenyl Chalcone Derivative Film. *J. At. Mol. Sci.* **2018**, *9*, 58–61. [[CrossRef](#)]
48. Rick, J.; Chou, T.-C. Using protein templates to direct the formation of thin-film polymer surfaces. *Biosens. Bioelectron.* **2006**, *22*, 544–549. [[CrossRef](#)] [[PubMed](#)]
49. Kang, E.-T.; Neoh, K.G.; Tan, K.L. Polyaniline: A polymer with many interesting intrinsic redox states. *Prog. Polym. Sci.* **1998**, *23*, 277–324. [[CrossRef](#)]
50. Long, Y.-Z.; Li, M.-M.; Gu, C.; Wan, M.; Duvail, J.-L.; Liu, Z.; Fan, Z. Recent advances in synthesis, physical properties and applications of conducting polymer nanotubes and nanofibers. *Prog. Polym. Sci.* **2011**, *36*, 1415–1442. [[CrossRef](#)]
51. Iwersen-Bergmann, S.; Schmoldt, A. Acute intoxication with aniline: Detection of acetaminophen as aniline metabolite. *Int. J. Leg. Med.* **2000**, *113*, 171–174. [[CrossRef](#)]
52. Khan, M.F.; Boor, P.J.; Gu, Y.; Alcock, N.W.; Ansari, G.A.S. Oxidative Stress in the Splenotoxicity of Aniline. *Fundam. Appl. Toxicol.* **1997**, *35*, 22–30. [[CrossRef](#)]
53. Gandarilla, A.M.D.; Matos, R.S.; Barcelay, Y.R.; da Fonseca Filho, H.D.; Brito, W.R. Molecularly imprinted polymer on indium tin oxide substrate for bovine serum albumin determination. *J. Polym. Res.* **2022**, *29*, 166. [[CrossRef](#)]
54. Lee, M.-H.; Thomas, J.L.; Liu, W.-C.; Zhang, Z.-X.; Liu, B.-D.; Yang, C.-H.; Lin, H.-Y. A multichannel system integrating molecularly imprinted conductive polymers for ultrasensitive voltammetric determination of four steroid hormones in urine. *Microchim. Acta* **2019**, *186*, 695. [[CrossRef](#)] [[PubMed](#)]
55. Roy, A.C.; Nisha, V.S.; Dhand, C.; Ali, M.A.; Malhotra, B.D. Molecularly imprinted polyaniline-polyvinyl sulphonic acid composite based sensor for para-nitrophenol detection. *Anal. Chim. Acta* **2013**, *777*, 63–71. [[CrossRef](#)]
56. Regasa, M.B.; Refera Soreta, T.; Femi, O.E.; Ramamurthy, P.C. Development of Molecularly Imprinted Conducting Polymer Composite Film-Based Electrochemical Sensor for Melamine Detection in Infant Formula. *ACS Omega* **2020**, *5*, 4090–4099. [[CrossRef](#)] [[PubMed](#)]
57. Lattach, Y.; Garnier, F.; Remita, S. Influence of Chemical and Structural Properties of Functionalized Polythiophene-Based Layers on Electrochemical Sensing of Atrazine. *ChemPhysChem* **2012**, *13*, 281–290. [[CrossRef](#)]
58. Lee, M.-H.; Liu, K.-T.; Thomas, J.L.; Su, Z.-L.; O'hare, D.; Van Wuellen, T.; Chamarro, J.M.; Bolognin, S.; Luo, S.-C.; Schwamborn, J.C.; et al. Peptide-Imprinted Poly(hydroxymethyl 3,4-ethylenedioxythiophene) Nanotubes for Detection of α Synuclein in Human Brain Organoids. *ACS Appl. Nano Mater.* **2020**, *3*, 8027–8036. [[CrossRef](#)]
59. Lach, P.; Cieplak, M.; Majewska, M.; Noworyta, K.R.; Sharma, P.S.; Kutner, W. “Gate Effect” in *p*-Synephrine Electrochemical Sensing with a Molecularly Imprinted Polymer and Redox Probes. *Anal. Chem.* **2019**, *91*, 7546–7553. [[CrossRef](#)] [[PubMed](#)]

60. Ayerdurai, V.; Cieplak, M.; Noworyta, K.R.; Gajda, M.; Ziminska, A.; Sosnowska, M.; Piechowska, J.; Borowicz, P.; Lisowski, W.; Shao, S.; et al. Electrochemical sensor for selective tyramine determination, amplified by a molecularly imprinted polymer film. *Bioelectrochemistry* **2021**, *138*, 107695. [[CrossRef](#)]
61. Yang, X.; Liu, H.; Ji, Y.; Xu, S.; Xia, C.; Zhang, R.; Zhang, C.; Miao, Z. A molecularly imprinted biosensor based on water-compatible and electroactive polymeric nanoparticles for lysozyme detection. *Talanta* **2022**, *236*, 122891. [[CrossRef](#)] [[PubMed](#)]
62. Sharma, P.S.; Iskierko, Z.; Noworyta, K.; Cieplak, M.; Borowicz, P.; Lisowski, W.; D'Souza, F.; Kutner, W. Synthesis and application of a "plastic antibody" in electrochemical microfluidic platform for oxytocin determination. *Biosens. Bioelectron.* **2018**, *100*, 251–258. [[CrossRef](#)]
63. Soysal, M. An Electrochemical Sensor Based on Molecularly Imprinted Polymer for Methyl Paraben Recognition and Detection. *J. Anal. Chem.* **2021**, *76*, 381–389. [[CrossRef](#)]
64. Ayankojo, A.G.; Reut, J.; Ciocan, V.; Öpik, A.; Syritski, V. Molecularly imprinted polymer-based sensor for electrochemical detection of erythromycin. *Talanta* **2020**, *209*, 120502. [[CrossRef](#)]
65. Ayankojo, A.G.; Reut, J.; Öpik, A.; Syritski, V. Sulfamethizole-imprinted polymer on screen-printed electrodes: Towards the design of a portable environmental sensor. *Sens. Actuators B Chem.* **2020**, *320*, 128600. [[CrossRef](#)]
66. Bartold, K.; Iskierko, Z.; Borowicz, P.; Noworyta, K.; Lin, C.-Y.; Kalecki, J.; Sharma, P.S.; Lin, H.-Y.; Kutner, W. Molecularly imprinted polymer-based extended-gate field-effect transistor (EG-FET) chemosensor for selective determination of matrix metalloproteinase-1 (MMP-1) protein. *Biosens. Bioelectron.* **2022**, *208*, 114203. [[CrossRef](#)] [[PubMed](#)]
67. Abbasy, L.; Mohammadzadeh, A.; Hasanzadeh, M.; Razmi, N. Development of a reliable bioanalytical method based on prostate specific antigen trapping on the cavity of molecular imprinted polymer towards sensing of PSA using binding affinity of PSA-MIP receptor: A novel biosensor. *J. Pharm. Biomed. Anal.* **2020**, *188*, 113447. [[CrossRef](#)] [[PubMed](#)]
68. Trevizan, H.F.; Olean-Oliveira, A.; Cardoso, C.X.; Teixeira, M.F.S. Development of a molecularly imprinted polymer for uric acid sensing based on a conductive azopolymer: Unusual approaches using electrochemical impedance/capacitance spectroscopy without a soluble redox probe. *Sens. Actuators B Chem.* **2021**, *343*, 130141. [[CrossRef](#)]
69. Syritski, V.; Reut, J.; Menaker, A.; Gyurcsányi, R.E.; Öpik, A. Electrosynthesized molecularly imprinted polypyrrole films for enantioselective recognition of l-aspartic acid. *Electrochim. Acta* **2008**, *53*, 2729–2736. [[CrossRef](#)]
70. Saidman, S.B. The effect of pH on the electrochemical polymerisation of pyrrole on aluminium. *J. Electroanal. Chem.* **2002**, *534*, 39–45. [[CrossRef](#)]
71. Liu, X.-X.; Zhang, L.; Li, Y.-B.; Bian, L.-J.; Su, Z.; Zhang, L.-J. Electropolymerization of aniline in aqueous solutions at pH 2 to 12. *J. Mater. Sci.* **2005**, *40*, 4511–4515. [[CrossRef](#)]
72. Meteleva-Fischer, Y.V.; Von Hauff, E.; Parisi, J. Electrochemical synthesis of polypyrrole layers doped with glutamic ions. *J. Appl. Polym. Sci.* **2009**, *114*, 4051–4058. [[CrossRef](#)]
73. Zhou, Q.; Shi, G. Conducting Polymer-Based Catalysts. *J. Am. Chem. Soc.* **2016**, *138*, 2868–2876. [[CrossRef](#)]
74. Shiigi, H.; Yakabe, H.; Kishimoto, M.; Kijima, D.; Zhang, Y.; Sree, U.; Deore, B.A.; Nagaoka, T. Molecularly Imprinted Overoxidized Polypyrrole Colloids: Promising Materials for Molecular Recognition. *Microchim. Acta* **2003**, *143*, 155–162. [[CrossRef](#)]
75. Kumpf, K.; Trattner, S.; Aspermaier, P.; Binting, J.; Fruhmann, P. P3HT and PEDOT: PSS printed thin films on chemiresistors: An economic and versatile tool for ammonia and humidity monitoring applications. *J. Appl. Polym. Sci.* **2023**, *140*, 53733. [[CrossRef](#)]
76. Bießmann, L.; Kreuzer, L.P.; Widmann, T.; Hohn, N.; Moulin, J.-F.; Müller-Buschbaum, P. Monitoring the Swelling Behavior of PEDOT:PSS Electrodes under High Humidity Conditions. *ACS Appl. Mater. Interfaces* **2018**, *10*, 9865–9872. [[CrossRef](#)] [[PubMed](#)]
77. Yin, F.; Mo, Y.; Liu, X.; Yang, H.; Zhou, D.; Cao, H.; Ye, T.; Xu, F. An ultra-sensitive and selective electrochemical sensor based on GOCS composite and ion imprinted polymer for the rapid detection of Cd²⁺ in food samples. *Food Chem.* **2023**, *410*, 135293. [[CrossRef](#)] [[PubMed](#)]
78. Bai, X.; Zhang, B.; Liu, M.; Hu, X.; Fang, G.; Wang, S. Molecularly imprinted electrochemical sensor based on polypyrrole/dopamine@graphene incorporated with surface molecularly imprinted polymers thin film for recognition of olaquinox. *Bioelectrochemistry* **2020**, *132*, 107398. [[CrossRef](#)] [[PubMed](#)]
79. Ma, X.; Gao, F.; Dai, R.; Liu, G.; Zhang, Y.; Lu, L.; Yu, Y. Novel electrochemical sensing platform based on a molecularly imprinted polymer-decorated 3D-multi-walled carbon nanotube intercalated graphene aerogel for selective and sensitive detection of dopamine. *Anal. Methods* **2020**, *12*, 1845–1851. [[CrossRef](#)]
80. Cai, D.; Ren, L.; Zhao, H.; Xu, C.; Zhang, L.; Yu, Y.; Wang, H.; Lan, Y.; Roberts, M.F.; Chuang, J.H.; et al. A molecular-imprint nanosensor for ultrasensitive detection of proteins. *Nat. Nanotechnol.* **2010**, *5*, 597–601. [[CrossRef](#)]
81. Ma, X.; Tu, X.; Gao, F.; Xie, Y.; Huang, X.; Fernandez, C.; Qu, F.; Liu, G.; Lu, L.; Yu, Y. Hierarchical porous MXene/amino carbon nanotubes-based molecular imprinting sensor for highly sensitive and selective sensing of fisetin. *Sens. Actuators B Chem.* **2020**, *309*, 127815. [[CrossRef](#)]
82. Wang, Z.; Li, H.; Chen, J.; Xue, Z.; Wu, B.; Lu, X. Acetylsalicylic acid electrochemical sensor based on PATP–AuNPs modified molecularly imprinted polymer film. *Talanta* **2011**, *85*, 1672–1679. [[CrossRef](#)]
83. Essousi, H.; Barhoumi, H.; Bibani, M.; Ktari, N.; Wendler, F.; Al-Hamry, A.; Kanoun, O. Ion-Imprinted Electrochemical Sensor Based on Copper Nanoparticles-Polyaniline Matrix for Nitrate Detection. *J. Sensors* **2019**, *2019*, 4257125. [[CrossRef](#)]
84. Mahmoud, A.M.; El-Wakil, M.M.; Mahnashi, M.H.; Ali, M.F.B.; Alkahtani, S.A. Modification of N,S co-doped graphene quantum dots with p-aminothiophenol-functionalized gold nanoparticles for molecular imprint-based voltammetric determination of the antiviral drug sofosbuvir. *Microchim. Acta* **2019**, *186*, 137–144. [[CrossRef](#)] [[PubMed](#)]

85. Duan, D.; Yang, H.; Ding, Y.; Li, L.; Ma, G. A three-dimensional conductive molecularly imprinted electrochemical sensor based on MOF derived porous carbon/carbon nanotubes composites and prussian blue nanocubes mediated amplification for chiral analysis of cysteine enantiomers. *Electrochim. Acta* **2019**, *302*, 137–144. [[CrossRef](#)]
86. Rezaei, B.; Khalili Boroujeni, M.; Ensafi, A.A. Caffeine electrochemical sensor using imprinted film as recognition element based on polypyrrole, sol-gel, and gold nanoparticles hybrid nanocomposite modified pencil graphite electrode. *Biosens. Bioelectron.* **2014**, *60*, 77–83. [[CrossRef](#)]
87. Komarova, E.; Aldissi, M.; Bogomolova, A. Design of molecularly imprinted conducting polymer protein-sensing films via substrate-dopant binding. *Anal.* **2015**, *140*, 1099–1106. [[CrossRef](#)] [[PubMed](#)]
88. Saumya, V.; Prathish, K.P.; Rao, T.P. In situ copper oxide modified molecularly imprinted polypyrrole film based voltammetric sensor for selective recognition of tyrosine. *Talanta* **2011**, *85*, 1056–1062. [[CrossRef](#)] [[PubMed](#)]
89. Mao, D.; Hu, J.; Duan, P.; Qin, C.; Piao, Y. Ultrasensitive and highly reusable electrochemical sensor with ion imprinted nanobiochar. *Sens. Actuators B Chem.* **2022**, *371*, 132490. [[CrossRef](#)]
90. Lee, M.-H.; Thomas, J.L.; Su, Z.-L.; Zhang, Z.-X.; Lin, C.-Y.; Huang, Y.-S.; Yang, C.-H.; Lin, H.-Y. Doping of transition metal dichalcogenides in molecularly imprinted conductive polymers for the ultrasensitive determination of 17 β -estradiol in eel serum. *Biosens. Bioelectron.* **2020**, *150*, 111901. [[CrossRef](#)]
91. Pandey, I.; Kant, R. Electrochemical impedance based chiral analysis of anti-ascorbic drug: L-Ascorbic acid and d -ascorbic acid using C-dots decorated conductive polymer nano-composite electrode. *Biosens. Bioelectron.* **2016**, *77*, 715–724. [[CrossRef](#)]
92. Lee, M.-H.; Liu, K.-H.; Thomas, J.L.; Chen, C.-Y.; Chen, C.-Y.; Yang, C.-H.; Lin, H.-Y. Doping of MXenes enhances the electrochemical response of peptide-imprinted conductive polymers for the recognition of C-Reactive protein. *Biosens. Bioelectron.* **2021**, *200*, 113930. [[CrossRef](#)]
93. Phonklam, K.; Wannapob, R.; Sriwimol, W.; Thavarungkul, P.; Phairatana, T. A novel molecularly imprinted polymer PMB/MWCNTs sensor for highly-sensitive cardiac troponin T detection. *Sens. Actuators B Chem.* **2020**, *308*, 127630. [[CrossRef](#)]
94. Yarkaeva, Y.; Maistrenko, V.; Dymova, D.; Zagitova, L.; Nazyrov, M. Polyaniline and poly(2-methoxyaniline) based molecular imprinted polymer sensors for amoxicillin voltammetric determination. *Electrochim. Acta* **2022**, *433*, 141222. [[CrossRef](#)]
95. Truta, L.A.A.N.A.; Sales, M.G.F. Carcinoembryonic antigen imprinting by electropolymerization on a common conductive glass support and its determination in serum samples. *Sens. Actuators B Chem.* **2019**, *287*, 53–63. [[CrossRef](#)]
96. Zhang, R.-R.; Gan, X.-T.; Xu, J.-J.; Pan, Q.-F.; Liu, H.; Sun, A.-L.; Shi, X.-Z.; Zhang, Z.-M. Ultrasensitive electrochemiluminescence sensor based on perovskite quantum dots coated with molecularly imprinted polymer for prometryn determination. *Food Chem.* **2022**, *370*, 131353. [[CrossRef](#)] [[PubMed](#)]
97. Teng, Y.; Fan, L.; Dai, Y.; Zhong, M.; Lu, X.; Kan, X. Electrochemical sensor for paracetamol recognition and detection based on catalytic and imprinted composite film. *Biosens. Bioelectron.* **2015**, *71*, 137–142. [[CrossRef](#)] [[PubMed](#)]
98. Abera, B.D.; Ortiz-Gómez, I.; Shkodra, B.; Romero, F.J.; Cantarella, G.; Petti, L.; Salinas-Castillo, A.; Lugli, P.; Rivadeneyra, A. Laser-Induced Graphene Electrodes Modified with a Molecularly Imprinted Polymer for Detection of Tetracycline in Milk and Meat. *Sensors* **2022**, *22*, 269. [[CrossRef](#)] [[PubMed](#)]
99. Tang, F.; Hua, Q.; Wang, X.; Luan, F.; Wang, L.; Li, Y.; Zhuang, X.; Tian, C. A novel electrochemiluminescence sensor based on a molecular imprinting technique and UCNPs@ZIF-8 nanocomposites for sensitive determination of imidacloprid. *Analyst* **2022**, *147*, 3917–3923. [[CrossRef](#)]
100. Wang, D.; Jiang, S.; Liang, Y.; Wang, X.; Zhuang, X.; Tian, C.; Luan, F.; Chen, L. Selective detection of enrofloxacin in biological and environmental samples using a molecularly imprinted electrochemiluminescence sensor based on functionalized copper nanoclusters. *Talanta* **2022**, *236*, 122835. [[CrossRef](#)]
101. Xie, C.; Li, H.; Li, S.; Wu, J.; Zhang, Z. Surface Molecular Self-Assembly for Organophosphate Pesticide Imprinting in Electropolymerized Poly(*p*-aminothiophenol) Membranes on a Gold Nanoparticle Modified Glassy Carbon Electrode. *Anal. Chem.* **2010**, *82*, 241–249. [[CrossRef](#)]
102. Lee, M.-H.; Thomas, J.L.; Su, Z.-L.; Yeh, W.-K.; Monzel, A.S.; Bolognin, S.; Schwamborn, J.C.; Yang, C.-H.; Lin, H.-Y. Transition metal dichalcogenides to optimize the performance of peptide-imprinted conductive polymers as electrochemical sensors. *Microchim. Acta* **2021**, *188*, 203. [[CrossRef](#)]
103. Moreira, L.F.P.P.; Buffon, E.; de Sá, A.C.; Stradiotto, N.R. Fructose determination in fruit juices using an electrosynthesized molecularly imprinted polymer on reduced graphene oxide modified electrode. *Food Chem.* **2021**, *352*, 129430. [[CrossRef](#)]
104. Wang, X.; Zheng, Y.; Xu, L. An electrochemical adenine sensor employing enhanced three-dimensional conductivity and molecularly imprinted sites of Au NPs bridged poly(3-thiophene acetic acid). *Sens. Actuators B Chem.* **2018**, *255*, 2952–2958. [[CrossRef](#)]
105. Liu, F.; Kan, X. Conductive imprinted electrochemical sensor for epinephrine sensitive detection and double recognition. *J. Electroanal. Chem.* **2019**, *836*, 182–189. [[CrossRef](#)]
106. Lach, P.; Cieplak, M.; Noworyta, K.R.; Pieta, P.; Lisowski, W.; Kalecki, J.; Chitta, R.; D'souza, F.; Kutner, W.; Sharma, P.S. Self-reporting molecularly imprinted polymer with the covalently immobilized ferrocene redox probe for selective electrochemical sensing of *p*-synephrine. *Sens. Actuators B Chem.* **2021**, *344*, 130276. [[CrossRef](#)]
107. Chen, S.; Shi, M.; Yang, J.; Yu, Y.; Xu, Q.; Xu, J.; Duan, X.; Gao, Y.; Lu, L. MXene/carbon nanohorns decorated with conductive molecularly imprinted poly(hydroxymethyl-3,4-ethylenedioxythiophene) for voltammetric detection of adrenaline. *Microchim. Acta* **2021**, *188*, 420. [[CrossRef](#)] [[PubMed](#)]

108. Lee, M.-H.; Lin, C.-C.; Kutner, W.; Thomas, J.L.; Lin, C.-Y.; Iskierko, Z.; Ku, Y.-S.; Lin, C.-Y.; Borowicz, P.; Sharma, P.S.; et al. Peptide-imprinted conductive polymer on continuous monolayer molybdenum disulfide transferred electrodes for electrochemical sensing of Matrix Metalloproteinase-1 in lung cancer culture medium. *Biosens. Bioelectron. X* **2023**, *13*, 100258. [[CrossRef](#)]
109. Sun, Y.; Xu, L.; Waterhouse, G.I.N.; Wang, M.; Qiao, X.; Xu, Z. Novel three-dimensional electrochemical sensor with dual signal amplification based on MoS₂ nanosheets and high-conductive NH₂-MWCNT@COF for sulfamerazine determination. *Sens. Actuators B Chem.* **2019**, *281*, 107–114. [[CrossRef](#)]
110. Moro, G.; Bottari, F.; Slegers, N.; Florea, A.; Cowen, T.; Moretto, L.M.; Piletsky, S.; De Wael, K. Conductive imprinted polymers for the direct electrochemical detection of B-lactam antibiotics: The case of cefquinome. *Sens. Actuators B Chem.* **2019**, *297*, 126786. [[CrossRef](#)]
111. Wang, X.; Dong, J.; Ming, H.; Ai, S. Sensing of glycoprotein via a biomimetic sensor based on molecularly imprinted polymers and graphene–Au nanoparticles. *Anal.* **2013**, *138*, 1219–1225. [[CrossRef](#)]
112. Martins, G.V.; Marques, A.C.; Fortunato, E.; Sales, M.G.F. Paper-based (bio)sensor for label-free detection of 3-nitrotyrosine in human urine samples using molecular imprinted polymer. *Sens. Bio-Sensing Res.* **2020**, *28*, 100333. [[CrossRef](#)]
113. Blinova, N.V.; Stejskal, J.; Trchová, M.; Prokeš, J.; Omastová, M. Polyaniline and polypyrrole: A comparative study of the preparation. *Eur. Polym. J.* **2007**, *43*, 2331–2341. [[CrossRef](#)]
114. Boeva, Z.A.; Sergeyev, V.G. Polyaniline: Synthesis, properties, and application. *Polym. Sci. Ser. C* **2014**, *56*, 144–153. [[CrossRef](#)]
115. Chen, Z.; Wright, C.; Dincel, O.; Chi, T.-Y.; Kameoka, J. A Low-Cost Paper Glucose Sensor with Molecularly Imprinted Polyaniline Electrode. *Sensors* **2020**, *20*, 1098. [[CrossRef](#)] [[PubMed](#)]
116. Singh, A.K.; Lakshmi, G.B.V.S.; Fernandes, M.; Sarkar, T.; Gulati, P.; Singh, R.P.; Solanki, P.R. A simple detection platform based on molecularly imprinted polymer for AFB1 and FuB1 mycotoxins. *Microchem. J.* **2021**, *171*, 106730. [[CrossRef](#)]
117. Liu, K.-H.; O'hare, D.; Thomas, J.L.; Guo, H.-Z.; Yang, C.-H.; Lee, M.-H. Self-assembly Synthesis of Molecularly Imprinted Polymers for the Ultrasensitive Electrochemical Determination of Testosterone. *Biosensors* **2020**, *10*, 16. [[CrossRef](#)]
118. Mohseni, E.; Yaftian, M.R.; Shayani-Jam, H.; Zamani, A.; Piri, F. Molecularly imprinted poly (4,4'-methylenedianiline) as electrochemical sensor for determination of 1-benzothiophene. *Synth. Met.* **2020**, *259*, 116252. [[CrossRef](#)]
119. Chuang, S.-W.; Rick, J.; Chou, T.-C. Electrochemical characterisation of a conductive polymer molecularly imprinted with an Amadori compound. *Biosens. Bioelectron.* **2009**, *24*, 3170–3173. [[CrossRef](#)]
120. Jahangiri-Manesh, A.; Mousazadeh, M.; Nikkhah, M. Fabrication of chemiresistive nanosensor using molecularly imprinted polymers for acetone detection in gaseous state. *Iran. Polym. J.* **2022**, *31*, 883–891. [[CrossRef](#)]
121. Jahangiri-Manesh, A.; Mousazadeh, M.; Nikkhah, M.; Abbasian, S.; Moshaii, A.; Masroor, M.J.; Norouzi, P. Molecularly imprinted polymer-based chemiresistive sensor for detection of nonanal as a cancer related biomarker. *Microchem. J.* **2022**, *173*, 106988. [[CrossRef](#)]
122. Alizadeh, T.; Rezaoo, F. Toluene chemiresistor sensor based on nano-porous toluene-imprinted polymer. *Int. J. Environ. Anal. Chem.* **2013**, *93*, 919–934. [[CrossRef](#)]
123. Alizadeh, T.; Rezaoo, F. A new chemiresistor sensor based on a blend of carbon nanotube, nano-sized molecularly imprinted polymer and poly methyl methacrylate for the selective and sensitive determination of ethanol vapor. *Sens. Actuators B Chem.* **2013**, *176*, 28–37. [[CrossRef](#)]
124. Alizadeh, T.; Hamedsoltani, L. Graphene/graphite/molecularly imprinted polymer nanocomposite as the highly selective gas sensor for nitrobenzene vapor recognition. *J. Environ. Chem. Eng.* **2014**, *2*, 1514–1526. [[CrossRef](#)]
125. Janfaza, S.; Banan Nojavani, M.; Nikkhah, M.; Alizadeh, T.; Esfandiar, A.; Ganjali, M.R. A selective chemiresistive sensor for the cancer-related volatile organic compound hexanal by using molecularly imprinted polymers and multiwalled carbon nanotubes. *Microchim. Acta* **2019**, *186*, 137. [[CrossRef](#)] [[PubMed](#)]
126. Halim, F.A.N.; Musa, N.H.; Zakaria, Z.; Kamarudin, S.F.; Noor, A.Y.M.; Derman, M.N.; Shakaff, A.Y.M. *Highly Sensitive Reduce Graphene Oxide—Molecular Imprinted Polymer Organic Thin Film Transistor for Serine Detection*; IEEE: Piscataway, NJ, USA, 2016; ISBN 9781509030286.
127. Halim, N.F.A.; Musa, N.H.; Zakaria, Z.; Von Schleusingen, M.; Ahmad, M.N.; Derman, N.; Shakaff, A.Y.M. Reduced graphene oxide/molecular imprinted polymer-organic thin film transistor for amino acid detection. In Proceedings of the 11th Asian Conference on Chemical Sensors: (ACCS2015), Penang, Malaysia, 16–18 November 2015; American Institute of Physics Inc.: College Park, MD, USA, 2015; Volume 1808. [[CrossRef](#)]
128. Zhang, Y.; Liu, Z.; Wang, Y.; Kuang, X.; Ma, H.; Wei, Q. Directly assembled electrochemical sensor by combining self-supported CoN nanoarray platform grown on carbon cloth with molecularly imprinted polymers for the detection of Tylosin. *J. Hazard. Mater.* **2020**, *398*, 122778. [[CrossRef](#)] [[PubMed](#)]
129. Li, Y.; Xu, W.; Zhao, X.; Huang, Y.; Kang, J.; Qi, Q.; Zhong, C. Electrochemical sensors based on molecularly imprinted polymers on Fe₃O₄/graphene modified by gold nanoparticles for highly selective and sensitive detection of trace ractopamine in water. *Analyst* **2018**, *143*, 5094–5102. [[CrossRef](#)]
130. Beigmoradi, F.; Rohani Moghadam, M.; Bazmandegan-Shamili, A.; Masoodi, H.R. Electrochemical sensor based on molecularly imprinted polymer coating on metal–organic frameworks for the selective and sensitive determination of carbendazim. *Microchem. J.* **2022**, *179*, 107633. [[CrossRef](#)]

131. Ge, L.; Chen, B.; Kawano, H.; Sassa, F.; Hayashi, K. Inkjet-printed Gas Sensor Matrix with Molecularly Imprinted Gas Selective Materials. In Proceedings of the IEEE Sensors, Montreal, QC, Canada, 27–30 October 2019; IEEE Sensors: Montreal, QC, Canada, 2019; Volume 2019, pp. 1–3. [\[CrossRef\]](#)
132. Shinohara, S.; Sassa, F.; Hayashi, K. Gas Selective Chemiresistor Composed of Molecularly Imprinted Polymer Composit Ink. In Proceedings of the 2016 IEEE Sensors, Orlando, FL, USA, 30 October–3 November 2016; Institute of Electrical and Electronics Engineers Inc.: Piscataway, NJ, USA, 2017.
133. Prasad, B.B.; Prasad, A.; Tiwari, M.P. Multiwalled carbon nanotubes-ceramic electrode modified with substrate-selective imprinted polymer for ultra-trace detection of bovine serum albumin. *Biosens. Bioelectron.* **2013**, *39*, 236–243. [\[CrossRef\]](#)
134. Wardani, N.I.; Kangkamano, T.; Wannapob, R.; Kanatharana, P.; Thavarungkul, P.; Limbut, W. Electrochemical sensor based on molecularly imprinted polymer cryogel and multiwalled carbon nanotubes for direct insulin detection. *Talanta* **2023**, *254*, 124137. [\[CrossRef\]](#)
135. Shao, Y.; Zhu, Y.; Zheng, R.; Wang, P.; Zhao, Z.; An, J. Highly sensitive and selective surface molecularly imprinted polymer electrochemical sensor prepared by Au and MXene modified glassy carbon electrode for efficient detection of tetrabromobisphenol A in water. *Adv. Compos. Hybrid Mater.* **2022**, *5*, 3104–3116. [\[CrossRef\]](#)
136. Wu, Y.; Deng, P.; Tian, Y.; Ding, Z.; Li, G.; Liu, J.; Zuberi, Z.; He, Q. Rapid recognition and determination of tryptophan by carbon nanotubes and molecularly imprinted polymer-modified glassy carbon electrode. *Bioelectrochemistry* **2020**, *131*, 107393. [\[CrossRef\]](#)
137. Antwi-Boampong, S.; Mani, K.S.; Carlan, J.; BelBruno, J.J. A selective molecularly imprinted polymer-carbon nanotube sensor for cotinine sensing. *J. Mol. Recognit.* **2013**, *27*, 57–63. [\[CrossRef\]](#)
138. Han, B.; Li, W.; Shen, Y.; Li, R.; Wang, M.; Zhuang, Z.; Zhou, Y.; Jing, T. Improving the sensitivity and selectivity of sulfonamides electrochemical detection with double-system imprinted polymers. *Sci. Total. Environ.* **2023**, *864*, 161173. [\[CrossRef\]](#) [\[PubMed\]](#)
139. Lee, S.P. Terpene Sensor Array with Bridge-Type Resistors by CMOS Technology. In Proceedings of the IOP Conference Series: Materials Science and Engineering; Institute of Physics Publishing, Bangalore, India, 16 July 2015; Volume 87.
140. Völkle, J.; Kumpf, K.; Feldner, A.; Lieberzeit, P.; Fruhmann, P. Development of conductive molecularly imprinted polymers (cMIPs) for limonene to improve and interconnect QCM and chemiresistor sensing. *Sens. Actuators B Chem.* **2022**, *356*, 131293. [\[CrossRef\]](#)
141. Koudehi, M.F.; Pourmortazavi, S.M. Polyvinyl Alcohol/Polypyrrole/Molecularly Imprinted Polymer Nanocomposite as Highly Selective Chemiresistor Sensor for 2,4-DNT Vapor Recognition. *Electroanalysis* **2018**, *30*, 2302–2310. [\[CrossRef\]](#)
142. Liang, Y.; Wang, H.; Xu, Y.; Pan, H.; Guo, K.; Zhang, Y.; Chen, Y.; Liu, D.; Zhang, Y.; Yao, C.; et al. A novel molecularly imprinted polymer composite based on polyaniline nanoparticles as sensitive sensors for parathion detection in the field. *Food Control* **2022**, *133*, 108638. [\[CrossRef\]](#)
143. Hassan, S.S.M.; Kamel, A.H.; Fathy, M.A. A novel screen-printed potentiometric electrode with carbon nanotubes/polyaniline transducer and molecularly imprinted polymer for the determination of nalbuphine in pharmaceuticals and biological fluids. *Anal. Chim. Acta* **2022**, *1227*, 340239. [\[CrossRef\]](#)
144. Harvey, D. *Modern Analytical Chemistry*; McGraw-Hill Higher Education: New York, NY, USA, 2000; Volume 816.
145. Antuña-Jiménez, D.; Díaz-Díaz, G.; Blanco-López, M.C.; Lobo-Castañón, M.J.; Miranda-Ordieres, A.J.; Tuñón-Blanco, P. Molecularly Imprinted Electrochemical Sensors: Past Present and Future. In *Molecularly Imprinted Sensors*; Elsevier: Amsterdam, The Netherlands, 2012; pp. 1–34. ISBN 9780444563316.
146. Hua, Y.; Ahmadi, Y.; Kim, K.-H. Molecularly imprinted polymers for sensing gaseous volatile organic compounds: Opportunities and challenges. *Environ. Pollut.* **2022**, *311*, 119931. [\[CrossRef\]](#)
147. Bräuer, B.; Unger, C.; Werner, M.; Lieberzeit, P.A. Biomimetic Sensors to Detect Bioanalytes in Real-Life Samples Using Molecularly Imprinted Polymers: A Review. *Sensors* **2021**, *21*, 5550. [\[CrossRef\]](#)
148. De Carvalho Silva, J.; Rodrigues, J.J.P.C.; Alberti, A.M.; Solic, P.; Aquino, A.L.L. LoRaWAN—A Low Power WAN Protocol for Internet of Things: A Review and Opportunities. In Proceedings of the 2017 2nd International Multidisciplinary Conference on Computer and Energy Science (SpliTech), Split, Croatia, 12–14 July 2017; Volume 2017, pp. 3–8.

Disclaimer/Publisher’s Note: The statements, opinions and data contained in all publications are solely those of the individual author(s) and contributor(s) and not of MDPI and/or the editor(s). MDPI and/or the editor(s) disclaim responsibility for any injury to people or property resulting from any ideas, methods, instructions or products referred to in the content.